

# ERROR BOUNDS FOR PHYSICS INFORMED NEURAL NETWORKS IN NONLINEAR SCHRÖDINGER EQUATIONS PLACED ON UNBOUNDED DOMAINS

MIGUEL Á. ALEJO, LUCREZIA COSSETTI, LUCA FANELLI, CLAUDIO MUÑOZ, AND NICOLÁS VALENZUELA

**ABSTRACT.** We consider the subcritical nonlinear Schrödinger (NLS) in dimension one posed on the unbounded real line. Several previous works have considered the deep neural network approximation of NLS solutions from the numerical and theoretical point of view in the case of bounded domains. In this paper, we introduce a new PINNs method to treat the case of unbounded domains and provide rigorous bounds on the associated approximation error in terms of the energy and Strichartz norms, provided a reasonable integration scheme is available. Applications to traveling waves, breathers and solitons, as well as numerical experiments confirming the validity of the approximation are also provided as well.

## 1. INTRODUCTION

**1.1. Setting.** Among deep learning methodologies studied in recent years, Physics Informed Neural Networks (PINN) technique has become one of the most relevant method to approximate solutions to physical models using neural networks. Originally proposed in [LLF98, LBH15, RaKa18, RPP19], the PINN technique uses the fact that deep artificial neural networks (DNNs hereafter) hold the property that any continuous, even measurable, function can be approximated by DNNs [Hor91, LLPS93, LLP00, LLF98, Yar17] (*universal approximation property*), but additionally uses the “physics” of the problem towards a better modeling of DNNs. Important examples and advances in this direction are given in [RaKa18, RPP19, PLK19, MJK20, Rai18, RPK17, RyMi22, KKLWY21]. PINNs have been also extended to cover elliptic PDEs [BDPS24, Zer22] and inverse problems [MiMo20, PeCh24]. Actually it is a dominant computational methodology applied to many research fields, ranging, without trying to be exhaustive, from General Relativity [FMR23, LNPC24, Had23], to discrete systems to unveil their underlying dynamical equations [SZC23, ZKCK22], to Quantum Mechanics [WaYa21, PLC21], to wave propagation [RHS22] and to fiber optics [ZYX22, ZFWCQ21]. Therefore the PINNs method allows one to use DNNs as ansatz spaces for the solutions of physically motivated PDEs.

In the whole context, various results show that for some classes of PDEs, deep neural networks succeed in approximating their solutions. Such results span from numerical to theoretical perspectives, with a wide range of applications. Among the PDEs studied with these methods and without being exhaustive, we find linear and semilinear parabolic equations [HJE18, HaJe17, HPW20, HJKW20b, BBGJJ21, BeJe19, JSW21], stochastic time dependent models [GHJW18, BeJe19, BGJ20], linear and semilinear time-independent elliptic equations [LLP00, GrHe21], a broad range of fluid equations [LMR20, MJK20, RJM22], and even time dependent/independent non-local equations [PLK19, GRPK19, GoSc21, Val22, Val23, Cas22] stand

---

2010 *Mathematics Subject Classification.* Primary 65K10, 65M99, Secondary: 68T07.

*Key words and phrases.* Nonlinear Schrödinger, Physics Informed Neural Networks, Deep Neural Networks, Unbounded Domains, Solitons.

M.Á.A. was partially supported by Grant PID2022-137228OB-I00 funded by the Spanish Ministerio de Ciencia, Innovación y Universidades, MICIU/AEI/10.13039/501100011033.

L. C. was supported by the grant Ramón y Cajal RYC2021-032803-I funded by MCIN/AEI/10.13039/50110 0011033 and by the European Union NextGenerationEU/PRTR, the Deutsche Forschungsgemeinschaft (DFG, German Research Foundation) – Project-ID 258734477 – SFB 1173 and by Ikerbasque.

L. F. was supported by the projects PID2021-123034NB-I00/MCIN/AEI/10.13039/501100011033 funded by the Agencia Estatal de Investigación, IT1615-22 funded by the Basque Government, and by Ikerbasque. He is also partially supported by the Basque Government through the BERC 2022–2025 program and by the Spanish Agencia Estatal de Investigación through BCAM Severo Ochoa excellence accreditation CEX2021-001142-S/MCIN/AEI/10.13039/501100011033.

C.M. was partially funded by Chilean research grants ANID 2022 Exploration 13220060, FONDECYT 1231250, and Basal CMM FB210005.

N.V. was partially funded by Chilean research grants ANID 2022 Exploration 13220060, FONDECYT 1231250, a Latin America PhD Google Fellowship and Basal CMM FB210005.

out. We refer to these works for further developments in this fast growing area of research. Additionally, one can classify the learning methods used to prove the previous results. Among the deep learning methods studied to date, and in addition to the PINN method described above, one can also find Montecarlo methods [Val22, Val23, MuVa24], Multilevel Picard Iterations (MLP) [HJKW20b, BH-JJK20], and even neural networks approximating infinite-dimensional operators, such as DeepOnets [ChCh95, LJK21, Cas23, CMV24], have been prominent. Other methods in the literature are for instance mentioned in the recent review [BHK23] and the monograph [JKW23].

Roughly speaking, PINNs profit of two important data that enjoy physical systems: initial and boundary conditions, although sometimes conserved quantities are also used. In the case of classical PDEs such as Schrödinger [BKM22], Burgers, Navier-Stokes, [RPK17, MJK20, RyMi22, RaKa18, LMR20, KMPT24], Kolmogorov [JSW21] and nonlinear diffusion through many phase materials [KK24], the PINNs method describes numerical approximations of classical solutions with accuracy.

PINNs in NLS models in bounded domains were already computed in the foundational work [RPP19]. One of the first rigorous results in this direction (i.e., using PINNs to approximate dispersive models in spatially-bounded domains) was obtained in [BKM22], based in previous work by Mishra and Molinaro [MiMo22]. Concerning wave models, in [MMN20] PINNs were used to solve the wave equation, and Montecarlo methods were generalized in [MuVa24]. Additionally, wave models were proved suitable for PINNs approximation in [LBK24] and even for approximating discontinuous solutions of PDEs appearing in nonlinear hyperbolic equations [RMM24]. However, not every physical model is placed in a bounded domain. For instance, solitonic solutions exist in dispersive equations placed on unbounded domains.

Consequently, one of the main concerns in some physical models of dispersive type is the lack of a bounded domain to ensure a global validity of the PINN method.

To overcome this domain representation's trouble, several improved PINNs or alternative neural networks have been proposed. In particular for solving infinite domain problems, a possible computational approach is to split the infinite domain into finite domain via absorption/ no-reflection boundary conditions [RRSL23, RRCWL24]. Another numerical methodology is to introduce a spectral expansion formulation [XBC23] for dealing with the infinite domain issue, and only using PINN to obtain the unknown coefficients in the spectral expansion formulation. Some other alternative approaches for dealing with unbounded domains in the case of seismic waves and thermal dynamics are [RRCWL24, BaEs22] respectively.

Here in this paper we propose a modification of the PINN technique that allows one to consider the case of unbounded problems, and we apply it to classical soliton solutions. For the sake of simplicity, we will focus ourself in a canonical one dimensional dispersive model that allows the existence of solitons and breathers: the one dimensional *focusing* NLS model posed in the (unbounded) real line:

$$i\partial_t u + \partial_x^2 u + |u|^{\alpha-1}u = 0, \quad (t, x) \in \mathbb{R} \times \mathbb{R}, \quad 2 \leq \alpha < \infty. \quad (1.1)$$

We assume complex-valued initial data  $u_0 \in H^1(\mathbb{R})$  and  $2 \leq \alpha < 5$ , which is the natural  $L^2$  subcritical case.\* Global in time solutions in  $H^1$  are well-known [GiVe79, GiVe85, Tsu87, Bou99, Caz03, Caz89, LiPo14], thanks to the conserved energy. Since no boundaries exist, we will replace the boundary data by *suitable global linear data*, in the following sense. Let  $I$  be a bounded time interval containing zero. Let

$$(p, q) = \left( \frac{4(\alpha+1)}{\alpha-1}, \alpha+1 \right)$$

be Schrödinger admissible pairs (see Definition 2.1). Let

- (1)  $f = f(x)$  be bounded differentiable, and  $g_n = g_n(t, x)$ ,  $n = 2, 3, 4$ , bounded and continuous, both complex-valued;
- (2) Integers  $N_1, N_2, N_3, N_4 \geq 1$ ,  $M_2, M_3, M_4 \geq 1$ ;
- (3) For  $n = 1, 2, 3, 4$ , collocation points  $(x_{n,j})_{j=1}^{N_n} \subseteq \mathbb{R}$ , and for  $n = 2, 3, 4$ , times  $(t_{n,\ell})_{\ell=1}^{M_n} \subseteq I$ ;
- (4) For  $n = 1, 2, 3, 4$ , vector weights  $(w_{n,j})_{j=1}^{N_n} \subseteq [0, 1]$ , and for  $n = 2, 3, 4$ , matrix weights  $(w_{n,\ell,j})_{\ell,j=1}^{M_n, N_n} \subseteq [0, 1]$ .

\*Some technical issues are present if  $\alpha < 2$ , but we believe that our results also apply to that case.

Consider the approximate norms

$$\begin{aligned}
\mathcal{J}_{H^1, N_1}[f] &:= \left( \frac{1}{N_1} \sum_{j=1}^{N_1} w_{1,j} (|f(x_j)|^2 + |f'(x_j)|^2) \right)^{1/2}, \\
\mathcal{J}_{\infty, H^1, N_2, M_2}[g_2] &:= \max_{\ell=1, \dots, M_2} \left( \frac{1}{N_2} \sum_{j=1}^{N_2} w_{2,\ell,j} (|g(t_{2,\ell}, x_{2,j})|^2 + |\partial_x g(t_{2,\ell}, x_{2,j})|^2) \right)^{1/2}, \\
\mathcal{J}_{p,q, N_3, M_3}[g_3] &:= \left( \frac{1}{M_3} \sum_{\ell=1}^{M_3} \left( \frac{1}{N_3} \sum_{j=1}^{N_3} w_{3,j,\ell} |g(t_{3,\ell}, x_{3,j})|^q \right)^{p/q} \right)^{1/p}, \\
\mathcal{J}_{p',q', N_4, M_4}[g_4] &:= \left( \frac{1}{M_4} \sum_{\ell=1}^{M_4} \left( \frac{1}{N_4} \sum_{j=1}^{N_4} w_{4,j,\ell} |g_4(t_{4,\ell}, x_{4,j})|^{q'} \right)^{p'/q'} \right)^{1/p'}.
\end{aligned} \tag{1.2}$$

The classical Riemann's sums are recovered with weights  $w_{n,j} = 1$  and  $w_{n,\ell,j} = 1$ . Usually, in numerical computations the colocation points and times will be chosen uniformly separated, emulating the simplest classical Riemann's sum. Our main result states that under smallness assumptions on  $\mathcal{J}_{H^1, N_1}$ ,  $\mathcal{J}_{p',q', N_4, M_4}$  of certain functions, PINNs approximate the NLS dynamics in unbounded domains in a satisfactory fashion.

**Hypotheses on integration schemes.** Following [MiMo22], our first requirement is a suitable way to approach integration.

(H1) Efficient integration. There exist efficient approximative rules for the computations of the  $H_x^1(\mathbb{R})$ ,  $L_t^\infty H_x^1(I \times \mathbb{R})$ ,  $L_t^p W_x^{1,q}(I \times \mathbb{R})$  and  $L_t^{p'} W_x^{1,q'}(I \times \mathbb{R})$  norms, in terms of the quantities defined in (1.2), in the following sense:

- For any  $\delta > 0$ , and all  $f \in H^1(\mathbb{R})$ , there exist  $N_1 \in \mathbb{N}$ ,  $R_1 > 0$ , points  $(x_{1,j})_{j=1}^{N_1} \subseteq [-R_1, R_1]$  and weights  $(w_{1,j})_{j=1}^{N_1} \subseteq [0, 1]$  such that

$$|\|f\|_{H^1(\mathbb{R})} - \mathcal{J}_{H^1, N_1}(f)| < \delta.$$

- For any  $\delta > 0$ , and all  $g_1 \in L_t^\infty H_x^1(I \times \mathbb{R})$ , there are  $N_2, M_2 \in \mathbb{N}$ ,  $R_2 > 0$ , points  $(t_{2,\ell}, x_{2,j})_{j=1}^{M_2, N_2} \subseteq I \times [-R_2, R_2]$  and weights  $(w_{2,\ell,j})_{\ell,j=1}^{M_2, N_2} \subseteq [0, 1]$  such that

$$|\|g_1\|_{L_t^\infty H_x^1(I \times \mathbb{R})} - \mathcal{J}_{\infty, H^1, N_2, M_2}(g_1)| < \delta.$$

- For any  $\delta > 0$ , and all  $g_3 \in L_t^p W_x^{1,q}(I \times \mathbb{R})$ , there are  $N_3, M_3 \in \mathbb{N}$ ,  $R_3 > 0$ , points  $(t_{3,\ell}, x_{3,j})_{j=1}^{M_3, N_3} \subseteq I \times [-R_3, R_3]$  and weights  $(w_{3,\ell,j})_{\ell,j=1}^{M_3, N_3} \subseteq [0, 1]$  such that

$$|\|g_3\|_{L_t^p W_x^{1,q}(I \times \mathbb{R})} - \mathcal{J}_{p,q, N_3, M_3}(g_3)| < \delta.$$

- For any  $\delta > 0$ , and all  $g_4 \in L_t^{p'} W_x^{1,q'}(I \times \mathbb{R})$ , there are  $N_4, M_4 \in \mathbb{N}$ ,  $R_4 > 0$ , points  $(t_{4,\ell}, x_{4,j})_{j=1}^{M_4, N_4} \subseteq I \times [-R_4, R_4]$  and weights  $(w_{4,\ell,j})_{\ell,j=1}^{M_4, N_4} \subseteq [0, 1]$  such that

$$|\|g_4\|_{L_t^{p'} W_x^{1,q'}(I \times \mathbb{R})} - \mathcal{J}_{p',q', N_4, M_4}(g_4)| < \delta.$$

Notice that even if we are considering functions defined in the full interval  $x \in \mathbb{R}$ , we profit of the fact that given any  $f$  of finite norm  $\|f\|_{H^1(\mathbb{R})} < +\infty$ , and tolerance  $\delta$ , it is possible to find  $R(\delta) > 0$  such that  $\|f\|_{H^1(|x| \geq R)} < \frac{1}{2}\delta$ . Therefore we can always restrict the *numerical integration* to a big finite interval  $[-R, R]$  (notice that this fact does not solve the problem of defining PINNs under boundary conditions at infinity). The same argument applies in the case of time-space norms. The previous requirements are also standard in the literature [MiMo22].

**Hypotheses on PINNs.** Let  $u_{\text{DNN},\#} = u_{\text{DNN},\#}(t, x)$  be a smooth bounded complex-valued function constructed by means of an algorithmic procedure (either SGD or any other ML optimization procedure) and realization of a suitable PINNs, in the following sense: under the framework (1.2), one has:

(H2) Uniformly bounded large time  $L_x^\infty H^1$ , initial time  $H_x^1$  and large time  $L_t^p W_x^{1,q}$  control for  $u_0$  and  $u_{\text{DNN},\#}$ . There are  $A, \tilde{A}, B > 0$  such that the following holds. For any  $N_{1,0}, N_{2,0}, N_{3,0} \geq 1$

and  $M_{2,0}, M_{3,0} \geq 1$ , there are  $N_j \geq N_{j,0}$  and  $M_j \geq M_{j,0}$  such that each approximate norm  $\mathcal{J}_{H^1, N_1}(u_0 - u_{\text{DNN}, \#}(0))$ ,  $\mathcal{J}_{\infty, H^1, N_2, M_2}[u_{\text{DNN}, \#}]$  and  $\mathcal{J}_{p,q, N_3, M_3}[u_{\text{DNN}, \#}]$  satisfies

$$\begin{aligned} \mathcal{J}_{H^1, N_1}(u_0 - u_{\text{DNN}, \#}(0)) &\leq \tilde{A}, \\ \mathcal{J}_{\infty, H^1, N_2, M_2}[u_{\text{DNN}, \#}] &\leq A, \quad \mathcal{J}_{p,q, N_3, M_3}[u_{\text{DNN}, \#}] \leq B. \end{aligned}$$

(H3) Small linear  $L_t^p W_x^{1,q}$  and nonlinear  $L_t^{p'} W_x^{1,q'}$  control. Given  $\varepsilon > 0$ , and given  $N_{4,0}, N_{5,0} \geq 1$  and  $M_{4,0}, M_{5,0} \geq 1$ , there are  $N_j \geq N_{j,0}$  and  $M_j \geq M_{j,0}$  and corresponding approximative norms  $\mathcal{J}_{p',q',N_4,M_4}[\mathcal{E}[u_{\text{DNN}, \#}]]$  and  $\mathcal{J}_{p,q,N_5,M_5}[e^{it\partial_x^2}(u_0 - u_{\text{DNN}, \#}(0))]$  such that

$$\mathcal{J}_{p',q',N_4,M_4}[\mathcal{E}[u_{\text{DNN}, \#}]] + \mathcal{J}_{p,q,N_5,M_5}[e^{it\partial_x^2}(u_0 - u_{\text{DNN}, \#}(0))] < \varepsilon,$$

with  $\mathcal{E}[u_{\#}] := i\partial_t u_{\#} + \partial_x^2 u_{\#} + |u_{\#}|^{\alpha-1} u_{\#}$ . Here  $e^{it\partial_x^2} f(x)$  represents the standard linear Schrödinger solution issued of initial data  $f$  at time  $t$  and position  $x$ .

Notice that  $u_{\text{DNN}, \#}$  may not be convergent to zero as time tends to infinity; then it is only required that, given a suitable tolerance  $\varepsilon$ , hypothesis (H3) is satisfied with computed data in the region  $[-R, R]$ , and with bounded local control given by (H2). Also, thanks to Strichartz estimates, the bound  $\mathcal{J}_{p,q,N_5,M_5}[e^{it\partial_x^2}(u_0 - u_{\text{DNN}, \#}(0))]$  may be obtained from  $\mathcal{J}_{H^1, N_1}(u_0 - u_{\text{DNN}, \#}(0)) \leq \tilde{A}$  by choosing  $\tilde{A}$  sufficiently small.

Finally, recall  $S'$  as the Strichartz space introduced in Definition 2.2.

**Theorem 1.1.** *Let  $u_0 \in H^1(\mathbb{R})$  be any given initial data. Assume (H1). Let  $A, \tilde{A}, B > 0$  be fixed numbers, and fix  $0 < \varepsilon < \varepsilon_1$  sufficiently small. Finally, let  $u_{\text{DNN}, \#}$  be a DNN satisfying (H2)-(H3). Then there exists a solution  $u \in S'(I \times \mathbb{R})$  to (1.1) on  $I \times \mathbb{R}$  with initial data  $u_0 \in H^1(\mathbb{R})$  such that for all  $R > 0$  sufficiently large and constants  $C$ ,*

$$\|u - u_{\text{DNN}, \#}\|_{L_t^p W_x^{1,q}(I \times [-R, R])} \leq C(A, \tilde{A}, B) \varepsilon, \quad (1.3)$$

$$\|u - u_{\text{DNN}, \#}\|_{S'(I \times [-R, R])} \leq C(A, \tilde{A}, B), \quad (1.4)$$

$$\|u - u_{\text{DNN}, \#}\|_{L_t^\infty H_x^1(I \times [-R, R])} \leq C(A, \tilde{A}, B). \quad (1.5)$$

The previous result states that PINNs satisfying bounds (H2) and (H3) will stay close in global norms to the solution of NLS. In particular, the  $L_t^p W_x^{1,q}(I \times [-R, R])$  norm stays small. The size of  $I$  is finite but arbitrary. Notice that smallness in the  $L_t^\infty H_x^1(I \times [-R, R])$  cannot be obtained unless  $\tilde{A}$  is chosen small. Additionally, since  $u_{\text{DNN}, \#}$  may not converge to zero as  $|x| \rightarrow \infty$ , conclusions stated within the interval  $[-R, R]$ , with  $R$  arbitrary but finite, are in some sense optimal.

Notice that the smallness condition (H3) on  $\mathcal{J}_{p',q',N_4,M_4}[\mathcal{E}[u_{\text{DNN}, \#}]]$  is standard when one studies PINNs. However, the smallness condition on  $\mathcal{J}_{p,q,N_3,M_3}[e^{it\partial_x^2}(u_0 - u_{\text{DNN}, \#}(0))]$  is one of the key new ingredients in this paper. It represents the fact that one requires that the *linear evolution* of close initial data should be controlled in a satisfactory way when tested via a PINNs method. This computation is easy to perform since linear evolution is quickly solved using current numerical methods and the fact that  $e^{it\partial_x^2} f$  is given by

$$\mathcal{F}_{\xi \rightarrow x}^{-1} \left( e^{-it\xi^2} \mathcal{F}_{x \rightarrow \xi}(f)(\xi) \right) = \frac{1}{(4i\pi t)^{1/2}} \int_y e^{-|x-y|^2/(4it)} f(y) dy,$$

with  $\mathcal{F}$  the standard Fourier transform. In particular,  $\mathcal{J}_{p,q,N_3,M_3}[e^{it\partial_x^2}(u_0 - u_{\text{DNN}, \#}(0))]$  can be easily estimated and computed. Moreover, if  $\tilde{A} = O(\varepsilon)$ , then the bound (H3) on  $\mathcal{J}_{p',q',N_4,M_4}[\mathcal{E}[u_{\text{DNN}, \#}]]$  is naturally satisfied. See Remark 3.1 for additional details.

An important advantage of Theorem 1.1 is the fact that the hypotheses are independent of the particular considered PINNs, meaning that classical and original definitions [LLF98, LBH15, RaKa18, RPP19] are as suitable as modern, latest contributions to the domain [PLC21, PLK19], among others.

Now we explain how Theorem 1.1 is proved. A key element will be a long-time stability property constructed specially for the mixing between DNNs and the NLS case. This stability property has been studied in great detail during previous years [TaVi05] as a tool to prove global well-posedness in critical equations, but in this case we have inspired us in this method and we have used them to propagate the PINNs restrictions in (H2)-(H3) to the full solution in the interval  $I \times [-R, R]$ , with  $R$  arbitrary. Moreover, Theorem 1.1 is still valid for any suitable DNN optimization method different to PINNs that satisfies (H1)-(H3) as well.

Finally, note that (4.2) may not be satisfactory since one also would like to have small  $L_t^\infty H_x^1$  norm on the error. This is naturally hard to ensure because of soliton/solitary wave solutions, which evolve in time moving energy from compact intervals towards infinity. Consequently, a good control will involve to generalize the standard orbital stability theory to the case of deep learning techniques. However, we are able to provide an interesting first result in this direction, see Corollary 6.1. More advances in this direction can be found in our forthcoming result [ACM24], where we use Montecarlo methods to control NLS, following our previous results for the wave equation [MuVa24].

**Organization of this work.** In Section 2 we provide some standard well-posedness results for NLS in  $H^1$ . In Section 3 we prove a short time stability result. In Section 4 we provide the main tool in this paper, a long time stability result. In Section 5 we prove the main results in this work. In Section 6 we provide numerical computations supporting our findings. Finally, in Section 7 we provide a discussion and conclusions.

**Acknowledgments.** C. M. would like to thank the Erwin Schrödinger Institute ESI (Vienna) where part of this work was written. N. V. thanks BCAM members for their hospitality and support during research visits in 2023 and 2024. M. Á. A. would like to thank the DIM-University of Chile, for its support and hospitality during research stays while this work was written.

## 2. WELL-POSEDNESS 1D-NLS WITH FOCUSING NONLINEARITY: $H^1$ THEORY

In this preliminary section we consider the Cauchy problem associated to the one dimensional NLS equation with focusing nonlinearity, namely (1.1). As customary, we show first *local* well-posedness of (1.1), then *global* well-posedness follows as an easy consequence of Gagliardo-Nirenberg inequalities. In our first result we show that the problem (1.1) is locally well-posed in  $H^1(\mathbb{R})$  for *any* power of the nonlinearity. In order to state the result we give the following preliminary definitions and we recall some useful result.

**Definition 2.1** (Admissible pairs). We say that a pair of exponents  $(p, q)$  is Schrödinger admissible if

$$\frac{2}{p} + \frac{n}{q} = \frac{n}{2}, \quad \begin{cases} 2 \leq q < \frac{2n}{n-2}, & \text{if } n \geq 3, \\ 2 \leq q < \infty, & \text{if } n = 2, \\ 2 \leq q \leq \infty, & \text{if } n = 1. \end{cases}$$

**Lemma 2.1** (Strichartz estimates). *Let  $(p, q)$  and  $(\tilde{p}, \tilde{q})$  Strichartz admissible pairs (cf. Definition 2.1), then the following estimates hold*

$$\|e^{it\Delta} f\|_{L_t^p L_x^q} \lesssim \|f\|_{L_x^2}, \quad (S1)$$

$$\left\| \int_{\mathbb{R}} e^{i(t-s)\Delta} g(\cdot, s) ds \right\|_{L_t^p L_x^q} \lesssim \|g\|_{L_t^{p'} L_x^{q'}}, \quad \left( \left\| \int_0^t e^{i(t-s)\Delta} g(\cdot, s) ds \right\|_{L_t^p L_x^q} \lesssim \|g\|_{L_t^{p'} L_x^{q'}} \right), \quad (S2)$$

$$\left\| \int_{\mathbb{R}} e^{it\Delta} g(\cdot, t) dt \right\|_{L_x^2} \lesssim \|g\|_{L_t^{p'} L_x^{q'}}. \quad (S3)$$

Combining (S2) and (S3) one gets

$$\left\| \int_0^t e^{i(t-s)\Delta} g(\cdot, s) ds \right\|_{L_t^p L_x^q} \lesssim \|g\|_{L_t^{\tilde{p}'} L_x^{\tilde{q}'}}. \quad (S4)$$

**Definition 2.2** (Strichartz space). Let  $I := [-T, T]$ . We define the  $\mathcal{S}'(I \times \mathbb{R})$  Strichartz norm by

$$\|u\|_{\mathcal{S}'(I \times \mathbb{R})} = \|u\|_{\mathcal{S}'} := \sup \|u\|_{L_t^p W_x^{1,q}(I \times \mathbb{R})},$$

where the supremum is taken over all 1D admissible pairs  $(p, q)$ . The associated Strichartz space  $\mathcal{S}'(I \times \mathbb{R})$  is defined as the closure of the test functions under this norm.

**Theorem 2.1** (Local well-posedness). *If  $1 < \alpha < \infty$ , then for all  $u_0 \in H^1(\mathbb{R})$  there exists  $T = T(\|u_0\|_{H^1(\mathbb{R})}, \alpha) > 0$  and a unique solution  $u$  of (1.1) in  $\mathcal{S}'(I \times \mathbb{R})$ .*

*Proof.* Let  $X_T$  denote the Strichartz space where to perform the fixed point argument. For all positive constants  $T$  and  $a$  we define  $B_T(0, a) = \{u \in X_T : \|u\|_{X_T} \leq a\}$ . For appropriate values of  $a$  and  $T > 0$  we shall show that

$$\Phi(u)(t) := e^{it\partial_x^2}u_0 + i \int_0^t e^{i(t-s)\partial_x^2}|u|^{\alpha-1}u \, ds, \quad t \in I$$

defines a contraction map on  $B_T(0, a)$ . In particular, if  $\Phi$  is proven to have the contracting property in  $X_T = \mathcal{S}'(I \times \mathbb{R})$ , then the result follows. To show that we proceed in three steps. We start considering as Strichartz space  $X_T$  the energy space  $X_T = L_t^\infty H_x^1(I \times \mathbb{R})$ .

**Case  $X_T = L_t^\infty H_x^1(I \times \mathbb{R})$ :** Due to the embedding  $H^1(\mathbb{R}) \hookrightarrow L^\infty(\mathbb{R})$  valid in the one dimensional framework, closing the fixed point argument in  $X_T$  is almost immediate. Indeed

$$\begin{aligned} \|\Phi(u)\|_{L_t^\infty H_x^1} &\leq \|e^{it\partial_x^2}u_0\|_{L_t^\infty H_x^1} + \left\| \int_0^t e^{i(t-s)\partial_x^2}|u|^{\alpha-1}u \, ds \right\|_{L_t^\infty H_x^1}, \\ &= \|u_0\|_{H_x^1} + \left\| \left\| \int_0^t e^{i(t-s)\partial_x^2}|u|^{\alpha-1}u \, ds \right\|_{H_x^1} \right\|_{L_t^\infty}, \end{aligned}$$

where here we just used that  $e^{it\partial_x^2}$  is unitary in  $H^1(\mathbb{R})$ . Using Minkowsky, the unitarity of  $e^{it\partial_x^2}$  and again the Sobolev embedding  $H^1(\mathbb{R}) \hookrightarrow L^\infty(\mathbb{R})$  one has

$$\begin{aligned} \left\| \int_0^t e^{i(t-s)\partial_x^2}|u|^{\alpha-1}u \, ds \right\|_{H_x^1} &\leq \int_0^t \| |u|^{\alpha-1}u \|_{H_x^1} \, ds \\ &\leq \int_0^t \|u\|_{H_x^1} \|u\|_{L^\infty}^{\alpha-1} \, ds \lesssim \int_0^t \|u\|_{H_x^1}^\alpha \, ds. \end{aligned}$$

Using the latter in the former one gets

$$\|\Phi(u)\|_{L_t^\infty H_x^1} \lesssim \|u_0\|_{H_x^1} + T \|u\|_{L_t^\infty H_x^1}^\alpha.$$

If we assume  $u \in B_T(0, a)$  in  $X_T = L_t^\infty H_x^1$ , namely  $\|u\|_{L_t^\infty H_x^1} \leq a$  and choosing  $a = 2c\|u_0\|_{H_x^1}$ , where  $c$  from now on will denote the constant hidden in the symbol  $\lesssim$ , then

$$\|\Phi(u)\|_{L_t^\infty H_x^1} \leq \frac{a}{2} + Ta^\alpha.$$

If  $T$  is sufficiently small, namely  $Ta^{\alpha-1} \leq 1/2$ , then  $\Phi: B_T(0, a) \rightarrow B_T(0, a)$ . Proving that  $\Phi$  is a contraction can be done similarly.

**Case  $X_T = L_t^\infty H_x^1 \cap L_t^{\frac{4(\alpha+1)}{\alpha-1}} W_x^{1,\alpha+1}$ :** <sup>†</sup> To close the fixed point argument in this case we need only to estimate the  $L_t^{\frac{4(\alpha+1)}{\alpha-1}} W_x^{1,\alpha+1}$ -norm of the Duhamel term. We shall see the estimate for  $\nabla u$ , the estimate for  $u$  is performed similarly. Using (S2) and Hölder in space one has

$$\begin{aligned} \left\| \int_0^t e^{it\partial_x^2}|u|^{\alpha-1}\nabla u \, ds \right\|_{L_t^{\frac{4(\alpha+1)}{\alpha-1}} L_x^{\alpha+1}} &\lesssim \| |u|^{\alpha-1}\nabla u \|_{L_t^{\frac{4(\alpha+1)}{3\alpha+5}} L_x^{\frac{\alpha+1}{\alpha}}} \\ &\leq \left\| \|\nabla u\|_{L_x^{\alpha+1}} \|u\|_{L_x^{\alpha+1}}^{\alpha-1} \right\|_{L_t^{\frac{4(\alpha+1)}{3\alpha+5}}}. \end{aligned}$$

Notice that since  $\alpha + 1 > 2$ , then  $H_x^1(\mathbb{R}) \hookrightarrow L_x^{\alpha+1}(\mathbb{R})$ . In particular,  $\|u\|_{L_x^{\alpha+1}} \leq \|u\|_{H^1}$ . Using Hölder in time gives

$$\begin{aligned} \left\| \|\nabla u\|_{L_x^{\alpha+1}} \|u\|_{L_x^{\alpha+1}}^{\alpha-1} \right\|_{L_t^{\frac{4(\alpha+1)}{3\alpha+5}}} &\leq \|u\|_{L_t^\infty H_x^1}^{\alpha-1} \|\nabla u\|_{L_t^{\frac{4(\alpha+1)}{3\alpha+5}} L_x^{\alpha+1}} \\ &\leq T^\delta \|u\|_{L_t^\infty H_x^1}^{\alpha-1} \|\nabla u\|_{L_t^{\frac{4(\alpha+1)}{\alpha-1}} L_x^{\alpha+1}} \\ &\leq T^\delta \|u\|_{X_T}^\alpha, \end{aligned}$$

here  $\delta$  is the Hölder conjugate exponent, namely

$$\frac{3\alpha+5}{4(\alpha+1)} = \frac{\alpha-1}{4(\alpha+1)} + \frac{1}{\delta}.$$

<sup>†</sup>The Strichartz space  $L_t^{\frac{4(\alpha+1)}{\alpha-1}} L_x^{\alpha+1}$  is the generalisation of  $L_t^8 L_x^4$  for the cubic nonlinearity  $\alpha = 3$ .

Notice that  $\delta > 0$ . This, with a similar reasoning as above, closes the fixed point argument. This intermediate step involving the Strichartz space  $L_t^{\frac{4(\alpha+1)}{\alpha-1}} L_x^{\alpha+1}$  is needed to treat the 1D admissible endpoint case which is object of the next step.

**Case  $X_T = L_t^\infty H_x^1 \cap L_t^4 W_x^{1,\infty}$ :** As above we need an estimate only for the Duhamel term. In order to do that we use the Strichartz estimate (S4) with  $(\tilde{p}, \tilde{q}) = (4(\alpha+1)/(3\alpha+5), (\alpha+1)/\alpha)$ . More precisely, using (S4) one has

$$\begin{aligned} \left\| \int_0^t e^{i(t-s)\partial_x^2} |u|^{\alpha-1} \nabla u \right\|_{L_t^4 L_x^\infty} &\lesssim \| |u|^{\alpha-1} \nabla u \|_{L_t^{\frac{4(\alpha+1)t}{3\alpha+5}} L_x^{\frac{\alpha+1}{\alpha}}} \\ &\lesssim T^\delta \| u \|_{L_t^\infty H_x^1}^{\alpha-1} \| \nabla u \|_{L_t^{\frac{4(\alpha+1)}{\alpha-1}} L_x^{\alpha+1}}, \end{aligned} \quad (2.1)$$

where the last inequality follows from the estimate obtained in the previous step. Now to conclude we want to use interpolation: let  $\theta \in (0, 1)$ , then

$$\begin{aligned} \|\nabla u\|_{L_x^{\alpha+1}} &= \left( \int_{\mathbb{R}} |\nabla u|^{(\alpha+1)\theta} |\nabla u|^{(\alpha+1)(1-\theta)} \right)^{1/(\alpha+1)} \\ &\leq \|\nabla u\|_{L_x^\infty}^{\frac{\alpha-1}{\alpha+1}} \|\nabla u\|_{L_x^2}^{\frac{2}{\alpha+1}}, \end{aligned}$$

where in the last estimate we used Hölder inequality and we chose  $\theta = 2/(\alpha+1)$ . Using the latter to estimate  $\|\nabla u\|_{L_t^{\frac{4(\alpha+1)}{\alpha-1}} L_x^{\alpha+1}}$  in (2.1) one has

$$\begin{aligned} \|\nabla u\|_{L_t^{\frac{4(\alpha+1)}{\alpha-1}} L_x^{\alpha+1}} &\leq \left\| \|\nabla u\|_{L_x^\infty}^{\frac{\alpha-1}{\alpha+1}} \|\nabla u\|_{L_x^2}^{\frac{2}{\alpha+1}} \right\|_{L_t^{\frac{4(\alpha+1)}{\alpha-1}}} \\ &\leq \|\nabla u\|_{L_t^\infty L_x^2}^{\frac{2}{\alpha+1}} \|\nabla u\|_{L_t^4 L_x^\infty}^{\frac{\alpha-1}{\alpha+1}} \leq \|u\|_{X_T}. \end{aligned}$$

Using the last estimate in (2.1) we easily close the fixed point argument.

In order to prove the theorem one observes that the pairs  $(\infty, 2)$  and  $(4, \infty)$  represent the endpoints of 1D admissible pairs  $(p, q)$ . Thus, the conclusion of the theorem simply follows from the interpolation inequality.  $\square$

### 3. SHORT TIME STABILITY

**3.1. Preliminaries.** We need the following preliminary definition.

**Definition 3.1** (Approximate solution). We say that  $u_\#$  is an approximate solution to the NLS model (1.1) if  $u_\#$  satisfies the perturbed equation

$$i\partial_t u_\# + \partial_x^2 u_\# + |u_\#|^{\alpha-1} u_\# = \mathcal{E}[u_\#], \quad 1 < \alpha < 5. \quad (3.1)$$

for some error function  $\mathcal{E}$ .

In this section we are interested in developing a *stability theory* for the NLS equation (1.1): we shall show that an approximate solution to the NLS equation (1.1) (in the sense of Definition 3.1) does not deviate too much from the solution of the actual model if the error function  $\mathcal{E}$  and the initial datum error are small in a suitable sense. In passing, notice that such a result generalises the continuous dependence of the data property, which corresponds to the special case  $\mathcal{E} = 0$  and the uniqueness property, which corresponds to the case  $\mathcal{E} = 0$  and zero initial datum error, namely  $u(0) = u_\#(0)$ .

**3.2. Short time stability.** As a first stability result we show that we can prove the existence of an exact solution  $u$  to (1.1) close enough to our approximate solution  $u_\#$  of (3.1), even allowing  $u_0 - u_\#(0)$  to have large energy, provided that the error  $\mathcal{E}[u_\#]$  of the near solution, the near solution  $u_\#$  itself and the free evolution of the perturbation  $u - u_\#$  are small in suitable space-time norms. The precise statement is contained in the next lemma.

**Lemma 3.1** (Short-time stability). *Let  $I$  be a fixed compact interval containing zero. Let  $u_\#$  be an approximate solution to (1.1) on  $I \times \mathbb{R}$  in the sense of Definition 3.1. Assume that  $\|u_\#\|_{L_t^\infty H_x^1(I \times \mathbb{R})} \leq A$ , for some constant  $A > 0$ . Let  $u_0 \in H^1(\mathbb{R})$  such that*

$$\|u_0 - u_\#(0)\|_{H^1(\mathbb{R})} \leq \tilde{A},$$

for some  $\tilde{A} > 0$ . Assume the smallness conditions

$$\|u_{\#}\|_{L_t^p W_x^{1,q}(I \times \mathbb{R})} \leq \varepsilon_0, \quad (3.2)$$

$$\|e^{it\partial_x^2}(u_0 - u_{\#}(0))\|_{L_t^p W_x^{1,q}(I \times \mathbb{R})} \leq \varepsilon, \quad (3.3)$$

$$\|\mathcal{E}[u_{\#}]\|_{L_t^{p'} W_x^{1,q'}(I \times \mathbb{R})} \leq \varepsilon, \quad (3.4)$$

for some  $0 < \varepsilon \leq \varepsilon_0$ , with  $\varepsilon_0 = \varepsilon_0(A, \tilde{A})$  a small constant and where  $(p, q) = \left(\frac{4(\alpha+1)}{\alpha-1}, \alpha+1\right)$ .

Then there exists a solution  $u \in \mathcal{S}'(I \times \mathbb{R})$  to (1.1) on  $I \times \mathbb{R}$  with initial datum  $u_0 \in H^1(\mathbb{R})$  such that

$$\|u - u_{\#}\|_{L_t^p W_x^{1,q}(I \times \mathbb{R})} \lesssim \varepsilon, \quad (3.5)$$

$$\|(i\partial_t + \partial_x^2)(u - u_{\#}) + \mathcal{E}[u_{\#}]\|_{L_t^{p'} W_x^{1,q'}(I \times \mathbb{R})} \lesssim \varepsilon \quad (3.6)$$

$$\|u - u_{\#}\|_{\mathcal{S}'(I \times \mathbb{R})} \lesssim \tilde{A} + \varepsilon. \quad (3.7)$$

In particular, from (3.7) one has  $\|u - u_{\#}\|_{L_t^{\infty} H_x^1(I \times \mathbb{R})} \lesssim \tilde{A} + \varepsilon$ .

*Remark 3.1.* Notice that from the Strichartz estimate (S1), the hypothesis (3.3) is redundant if one is willing to assume also smallness of the energy of  $u_0 - u_{\#}(0)$ , namely asking  $\tilde{A} = \mathcal{O}(\varepsilon)$ .

*Proof of Lemma 3.1.* By the well-posedness theory developed in the previous section (Theorem 2.1), we can assume that the solution  $u$  to (1.1) already exists and belongs to  $\mathcal{S}'$ . Thus to prove the result we need only to show (3.5)-(3.7) as a priori estimates. We establish these bounds for  $t \geq 0$ , the portion of  $I$  corresponding to  $t_0 < 0$  can be treated similarly.

Let  $v := u - u_{\#}$ . Then  $v$  satisfies the following equation

$$i\partial_t v + \partial_x^2 v + f(u_{\#} + v) - f(u_{\#}) + \mathcal{E}[u_{\#}] = 0, \quad f(s) := |s|^{\alpha-1} s. \quad (3.8)$$

Using the integral equation associated to (3.8) one has

$$v(t) = e^{it\partial_x^2}(u_0 - u_{\#}(0)) + i \int_0^t e^{i(t-s)\partial_x^2} [f(u_{\#} + v) - f(u_{\#})] ds + i \int_0^t e^{i(t-s)\partial_x^2} \mathcal{E}[u_{\#}] ds. \quad (3.9)$$

Let  $T \in I$ , we will now work on the slab  $[0, T] \times \mathbb{R}$ .

Using (S1) for the first term in (3.9), (S2) for the second and the third terms and then hypotheses (3.2) and (3.4) we have

$$\begin{aligned} \|v\|_{\mathcal{S}'} &\lesssim \|u_0 - u_{\#}(0)\|_{H_x^1} + \|f(u_{\#} + v) - f(u_{\#})\|_{L_t^{p'} W_x^{1,q'}} + \|\mathcal{E}[u_{\#}]\|_{L_t^{\tilde{p}'} W_x^{1,\tilde{q}'}} \\ &\lesssim \tilde{A} + S(T) + \varepsilon, \end{aligned} \quad (3.10)$$

where we have defined

$$S(T) := \|f(u_{\#} + v) - f(u_{\#})\|_{L_t^{p'} W_x^{1,q'}([0, T] \times \mathbb{R})}.$$

Using that  $f(s) = |s|^{\alpha-1} s$  one easily has

$$|\nabla[f(u_{\#} + v) - f(u_{\#})]| \lesssim |\nabla u_{\#}| |v|^{\alpha-1} + |\nabla v| |u_{\#}|^{\alpha-1} + |\nabla v| |v|^{\alpha-1}, \quad (3.11)$$

(for example, see [TaVi05]). Thus, in order to bound  $S(t)$  we need to estimate terms of the following type  $\|u|^{\alpha-1} \nabla u\|_{L_t^{p'} L_x^{q'}}$ . Using the Hölder inequality one obtains

$$\begin{aligned} \|u|^{\alpha-1} \nabla u\|_{L_t^{p'} L_x^{q'}} &= \|u|^{\alpha-1} \nabla u\|_{L_t^{\frac{4(\alpha+1)}{3\alpha+5}} L_x^{\frac{\alpha+1}{\alpha}}} \leq \|\nabla u\|_{L_x^{\alpha+1}} \|u\|_{L_x^{\alpha+1}}^{\alpha-1} \|u\|_{L_t^{\frac{4(\alpha+1)}{3\alpha+5}}} \\ &\leq \|\nabla u\|_{L_t^{\frac{4(\alpha+1)}{\alpha-1}} L_x^{\alpha+1}} \|u\|_{L_t^{\frac{2(\alpha^2-1)}{\alpha+3}} L_x^{\alpha+1}}^{\alpha-1} \\ &\leq T^{\delta} \|\nabla u\|_{L_t^{\frac{4(\alpha+1)}{\alpha-1}} L_x^{\alpha+1}} \|u\|_{L_t^{\frac{4(\alpha+1)}{\alpha-1}} L_x^{\alpha+1}}^{\alpha-1} \\ &\leq T^{\delta} \|\nabla u\|_{L_t^p L_x^q} \|u\|_{L_t^p L_x^q}^{\alpha-1}, \end{aligned} \quad (3.12)$$

where  $\delta$  is a Hölder conjugate exponent which is positive if  $\alpha < 5$  being  $\frac{2(\alpha^2-1)}{\alpha+3} < \frac{4(\alpha+1)}{\alpha-1}$ . Using (3.11) and (3.12) it follows

$$\begin{aligned} S(T) &\lesssim \|\nabla u_\#|v|^{\alpha-1}\|_{L_t^{p'} L_x^{q'}} + \|\nabla v|u_\#|^{\alpha-1}\|_{L_t^{p'} L_x^{q'}} + \|\nabla v|v|^{\alpha-1}\|_{L_t^{p'} L_x^{q'}} \\ &\lesssim_T \|\nabla u_\#|L_t^p L_x^q\|v\|_{L_t^p L_x^q}^{\alpha-1} + \|\nabla v\|_{L_t^p L_x^q}\|u_\#\|_{L_t^p L_x^q}^{\alpha-1} + \|\nabla v\|_{L_t^p L_x^q}\|v\|_{L_t^p L_x^q}^{\alpha-1} \\ &\lesssim_T \|u_\#\|_{L_t^p W_x^{1,q}}\|v\|_{L_t^p W_x^{1,q}}^{\alpha-1} + \|v\|_{L_t^p W_x^{1,q}}\|u_\#\|_{L_t^p W_x^{1,q}}^{\alpha-1} + \|v\|_{L_t^p W_x^{1,q}}^\alpha. \end{aligned} \quad (3.13)$$

Using (3.2) and that

$$\begin{aligned} \|v\|_{L_t^p W_x^{1,q}} &\lesssim \|e^{it\partial_x^2}(u_0 - u_\#(0))\|_{L_t^p W_x^{1,q}} + \|f(u_\# + v) - f(u_\#)\|_{L_t^{p'} W_x^{1,q'}} + \|\mathcal{E}[u_\#]\|_{L_t^{p'} W_x^{1,q'}} \\ &\lesssim S(T) + \varepsilon, \end{aligned} \quad (3.14)$$

where in the last inequality we have used (3.3) and (3.4), from (3.13) we have

$$S(T) \lesssim_T \varepsilon_0(S(T) + \varepsilon)^{\alpha-1} + \varepsilon_0^{\alpha-1}(S(T) + \varepsilon) + (S(T) + \varepsilon)^\alpha.$$

Taking  $\varepsilon_0$  sufficiently small, a standard continuity argument gives

$$S(T) \leq \varepsilon, \quad \text{for all } T \in I,$$

which implies (3.6). Using this bound in (3.14) and (3.10) gives (3.5) and (3.7), respectively. Thus the proof of the lemma is concluded.  $\square$

#### 4. LONG TIME STABILITY

We will actually be interested in iterating the above result to deal with the more general situation of near-solutions with *finite* but *arbitrarily large* space-time norms. More precisely, we are interested in proving the following alternative lemma.

**Lemma 4.1** (Long-time stability). *Let  $I$  be a fixed compact interval containing zero. Let  $u_\#$  be an approximate solution to (1.1) on  $I \times \mathbb{R}$  in the sense of Definition 3.1. Assume that*

$$\|u_\#\|_{L_t^\infty H_x^1(I \times \mathbb{R})} \leq A, \quad (4.1)$$

for some constant  $A > 0$ . Let  $u_0 \in H^1(\mathbb{R})$  such that

$$\|u_0 - u_\#(0)\|_{H^1(\mathbb{R})} \leq \tilde{A}, \quad (4.2)$$

for some  $\tilde{A} > 0$ . Assume

$$\|u_\#\|_{L_t^p W_x^{1,q}(I \times \mathbb{R})} \leq B, \quad (4.3)$$

$$\|e^{it\partial_x^2}(u_0 - u_\#(0))\|_{L_t^p W_x^{1,q}(I \times \mathbb{R})} \leq \varepsilon, \quad (4.4)$$

$$\|\mathcal{E}[u_\#]\|_{L_t^{p'} W_x^{1,q'}(I \times \mathbb{R})} \leq \varepsilon, \quad (4.5)$$

for some constant  $B > 0$ ,  $0 < \varepsilon \leq \varepsilon_1$ , with  $\varepsilon_1 = \varepsilon_1(A, \tilde{A}, B) > 0$  a small constant, where  $(p, q) = \left(\frac{4(\alpha+1)}{\alpha-1}, \alpha+1\right)$ .

Then there exists a unique solution  $u \in \mathcal{S}'(I \times \mathbb{R})$  to (1.1) on  $I \times \mathbb{R}$  with initial data  $u_0 \in H^1(\mathbb{R})$  such that

$$\|u - u_\#\|_{L_t^p W_x^{1,q}(I \times \mathbb{R})} \leq C(A, \tilde{A}, B)\varepsilon, \quad (4.6)$$

$$\|u - u_\#\|_{\mathcal{S}'(I \times \mathbb{R})} \leq C(A, \tilde{A}, B). \quad (4.7)$$

In particular, from (4.7) one has  $\|u - u_\#\|_{L_t^\infty H_x^1(I \times \mathbb{R})} \leq C(A, \tilde{A}, B)$ .

Lemma 4.1 can be obtained as an easy consequence of Lemma 3.1 just using an iteration argument based on partitioning the time interval.

*Proof of Lemma 4.1.* With no loss of generality we may assume that  $t_0 := 0$  is the lower bound of the interval  $I$ . Let  $\varepsilon_0 = \varepsilon_0(A, 2\tilde{A})$  be as in Lemma 3.1. Since from (4.3) the  $L_t^p W_x^{1,q}(I \times \mathbb{R})$  norm of  $u_\#$  is finite, we can subdivide the interval  $I$  into  $N \leq C(A, B, \varepsilon_0)$  sub-intervals  $I_j = [t_j, t_{j+1}]$  such that on each  $I_j$  we have

$$\|u_\#\|_{L_t^p W_x^{1,q}(I_j \times \mathbb{R})} \leq \varepsilon_0. \quad (4.8)$$

Choosing  $\varepsilon_1$  sufficiently small depending on  $\varepsilon_0, N, A$  and  $\tilde{A}$ , we can apply Lemma 3.1 to obtain that for each  $j \in \{0, \dots, N-1\}$  then we have

$$\begin{aligned} \|u - u_{\#}\|_{L_t^p W_x^{1,q}(I_j \times \mathbb{R})} &\lesssim_j \varepsilon, \\ \|u - u_{\#}\|_{\mathcal{S}'(I_j \times \mathbb{R})} &\lesssim_j \tilde{A} + \varepsilon, \end{aligned} \quad (4.9)$$

provided we can show that the smallness assumptions (4.4) and (4.5) hold with  $t_0 = 0$  replaced by the lower bound  $t_j$  of the sub-interval  $I_j$ . First of all one observes that by an inductive argument

$$S(t_l) := \|(i\partial_t + \partial_x^2)(u - u_{\#}) + \mathcal{E}[u_{\#}]\|_{L_t^p W_x^{1,q}(I_l \times \mathbb{R})} \leq C(l)\varepsilon,$$

for any  $l \in \{0, N-1\}$ . From Lemma 3.1 applied to  $I_0 = [0, t_1]$ , one has  $S(t_0) \leq \varepsilon$  (cf. (3.6)). Arguing as in the proof of Lemma 3.1, for  $l \in \{1, N-1\}$  we get

$$S(t_l) \leq \sum_{k=1}^{\alpha} \|v\|_{L_t^p W_x^{1,q}([0, t_{l+1}] \times \mathbb{R})}^k \|u_{\#}\|_{L_t^p W_x^{1,q}(I_l \times \mathbb{R})}^{\alpha-k}. \quad (4.10)$$

From the integral equation (3.9) one has

$$\begin{aligned} &\|v\|_{L_t^p W_x^{1,q}([0, t_{l+1}] \times \mathbb{R})} \\ &\leq \|e^{it\partial_x^2}(u_0 - u_{\#}(0))\|_{L_t^p W_x^{1,q}([0, t_{l+1}] \times \mathbb{R})} + \|(i\partial_t + \partial_x^2)(u - u_{\#}) + \mathcal{E}[u_{\#}]\|_{L_t^{p'} W_x^{1,q'}([0, t_{l+1}] \times \mathbb{R})} + \|\mathcal{E}[u_{\#}]\|_{L_t^{p'} W_x^{1,q'}(I \times \mathbb{R})} \\ &\leq \|e^{it\partial_x^2}(u_0 - u_{\#}(0))\|_{L_t^p W_x^{1,q}([0, t_{l+1}] \times \mathbb{R})} + \sum_{m=0}^{l-1} S(t_m) + S(t_l) + \|\mathcal{E}[u_{\#}]\|_{L_t^{p'} W_x^{1,q'}(I \times \mathbb{R})} \\ &\leq C(l)(S(t_l) + \varepsilon), \end{aligned}$$

where the last bound follows from (4.4), (4.5) and the inductive hypothesis  $S(t_m) \leq C(m)\varepsilon$  for any  $m \in \{0, l-1\}$ . Plugging this bound in (4.10), using also (4.8), then a continuity argument as above gives

$$S(t_l) \leq C(l)\varepsilon. \quad (4.11)$$

Now, using (3.9), by the unitarity in  $H_x^1$  of the operator  $e^{it\partial_x^2}$  and from Strichartz estimate (S4) one has

$$\begin{aligned} \|u(t_j) - u_{\#}(t_j)\|_{H_x^1(\mathbb{R})} &\leq \|u(t) - u_{\#}(t)\|_{L_t^{\infty} H_x^1([0, t_j] \times \mathbb{R})} \\ &\leq \|u_0 - u_{\#}(0)\|_{H_x^1(\mathbb{R})} + \sum_{l=0}^{j-1} S(t_l) + \|\mathcal{E}[u_{\#}]\|_{L_t^{p'} W_x^{1,q'}(I \times \mathbb{R})} \\ &\lesssim \tilde{A} + \varepsilon + \sum_{l=0}^{j-1} C(l)\varepsilon, \end{aligned}$$

where the last bound follows from (4.2), (4.5) and (4.11).

Similarly, one has

$$\begin{aligned} &\|e^{i(t-t_j)\partial_x^2}(u(t_j) - u_{\#}(t_j))\|_{L_t^p W_x^{1,q}(I_j \times \mathbb{R})} \\ &\leq \|e^{it\partial_x^2}(u_0 - u_{\#}(0))\|_{L_t^p W_x^{1,q}([0, t_{j+1}] \times \mathbb{R})} + \left\| \int_0^{t_j} e^{i(t-s)\partial_x^2}(i\partial_t + \partial_x^2)(u - u_{\#}) ds \right\|_{L_t^p W_x^{1,q}([0, t_{j+1}] \times \mathbb{R})} \\ &\leq \|e^{it\partial_x^2}(u_0 - u_{\#}(0))\|_{L_t^p W_x^{1,q}([0, t_{j+1}] \times \mathbb{R})} + \sum_{l=0}^j S(t_l) + \|\mathcal{E}[u_{\#}]\|_{L_t^{p'} W_x^{1,q'}(I \times \mathbb{R})} \\ &\leq \varepsilon + \sum_{l=0}^j C(l)\varepsilon. \end{aligned}$$

Choosing  $\varepsilon_1$  sufficiently small, one has that (4.9) holds true for any  $j \in \{0, \dots, N-1\}$ . Thus, bounds (4.6) and (4.7) follow summing over all the intervals  $I_j$ ,  $j \in \{0, \dots, N-1\}$ .  $\square$

## 5. PROOF OF THE MAIN RESULT

Consider an interval of time  $I$  containing zero. Let  $u_0 \in H^1(\mathbb{R})$ . Assume (H1). Let  $A, \tilde{A}, B > 0$  be fixed values. Let  $0 < \varepsilon < \varepsilon_1(A, \tilde{A}, B)$ . Recall

$$(p, q) = \left( \frac{4(\alpha+1)}{\alpha-1}, \alpha+1 \right).$$

Let  $u(t)$  be the corresponding solution to NLS with initial data  $u_0$ . Let  $u_{\text{DNN},\#}$  be the realization of a DNN  $\Phi_\#$  as in Theorem 1.1, such that (H2) and (H3) are satisfied in the following sense:

(Step 1) For  $N_1, N_2, N_3$  and  $M_2, M_3$  sufficiently large, collocation points, times and weights, one has

$$\mathcal{J}_{\infty, H^1, N_2, M_2}[u_{\text{DNN},\#}] \leq \frac{1}{2}A, \quad \mathcal{J}_{H^1, N_1}(u_0 - u_{\text{DNN},\#}(0)) \leq \frac{1}{2}\tilde{A}, \quad \mathcal{J}_{p, q, N_3, M_3}[u_{\text{DNN},\#}] \leq \frac{1}{2}B.$$

Later we will choose specific values for the parameters of the approximative norms. Similarly, we will require as well that

(Step 2) For all  $N_4, M_4$  and  $N_5, M_5$  positive integers large enough, collocation points, times and weights,

$$\mathcal{J}_{p', q', N_4, M_4}[\mathcal{E}[u_{\text{DNN},\#}]] + \mathcal{J}_{p, q, N_5, M_5}[e^{it\partial_x^2}(u_0 - u_{\text{DNN},\#}(0))] < \frac{1}{2}\varepsilon,$$

$$\text{with } \mathcal{E}[u_\#] := i\partial_t u_\# + \partial_x^2 u_\# + |u_\#|^{\alpha-1} u_\#.$$

Let

$$R := \max_{n=1,2,3,4} \max_{j=1,\dots,N_1} \{|x_{n,j}| \}$$

be the maximum modulus of evaluation/collocation points among all the previous approximate integrals. Let  $[-R, R] \subseteq \mathbb{R}$ . Let  $\eta_R \in C_0^\infty(\mathbb{R})$ ,  $0 \leq \eta \leq 1$ , be a cut-off function such that  $\eta = 1$  in  $[-R, R]$  and  $\eta(x) = 0$  if  $|x| \geq 2R$ . Define  $u_\# := u_{\text{DNN},\#} \eta_R$  now in Sobolev and Lebesgue spaces. Note that for all  $t \in I$ , and all  $x \in [-R, R]$ , one has  $u_\# = u_{\text{DNN},\#}$ . Consequently,

$$\begin{aligned} \mathcal{J}_{\infty, H^1, N_2, M_2}[u_{\text{DNN},\#}] &= \mathcal{J}_{\infty, H^1, N_2, M_2}[u_\#], \\ \mathcal{J}_{H^1, N_1}(u_0 - u_{\text{DNN},\#}(0)) &= \mathcal{J}_{H^1, N_1}(u_0 - u_\#(0)), \quad \mathcal{J}_{p, q, N_3, M_3}[u_{\text{DNN},\#}] = \mathcal{J}_{p, q, N, M}[u_\#], \end{aligned}$$

and

$$\begin{aligned} \mathcal{J}_{p', q', N_4, M_4}[\mathcal{E}[u_{\text{DNN},\#}]] &= \mathcal{J}_{p', q', N_4, M_4}[\mathcal{E}[u_\#]], \\ \mathcal{J}_{p, q, N_5, M_5}[e^{it\partial_x^2}(u_0 - u_{\text{DNN},\#}(0))] &= \mathcal{J}_{p, q, N_5, M_5}[e^{it\partial_x^2}(u_0 - u_\#(0))]. \end{aligned}$$

Now (modulo choosing  $N_j, M_j$  once again larger, and  $R$  larger if necessary, which does not affect the last identities) we can use hypothesis (H1) and choose particular integration parameters for  $f = u_0 - u_\#(0)$  and  $\delta = \frac{1}{2}\varepsilon$  to get

$$\|u_0 - u_\#(0)\|_{H^1(\mathbb{R})} \leq \mathcal{J}_{H^1, N_1}(u_0 - u_\#(0)) + \frac{1}{2}\varepsilon.$$

Similarly, for  $g_2 = g_3 = u_\#$  and  $\delta = \frac{1}{2}\varepsilon$ , we choose integration parameters such that

$$\begin{aligned} \|u_\#\|_{L_t^\infty H^1(I \times \mathbb{R})} &\leq \mathcal{J}_{\infty, H^1, N_2, M_2}[u_\#] + \frac{1}{2}\varepsilon, \\ \|u_\#\|_{L_t^p W_x^{1,q}(I \times \mathbb{R})} &\leq \mathcal{J}_{p, q, N_3, M_3}[u_\#] + \frac{1}{2}\varepsilon. \end{aligned}$$

Therefore,

$$\begin{aligned} \|u_0 - u_\#(0)\|_{H^1(\mathbb{R})} &\leq \mathcal{J}_{H^1, N_1}(u_0 - u_{\text{DNN},\#}(0)) + \frac{1}{2}\varepsilon \leq \frac{1}{2}(\tilde{A} + \varepsilon) \leq \tilde{A}, \\ \|u_\#\|_{L_t^\infty H^1(I \times \mathbb{R})} &\leq \mathcal{J}_{\infty, H^1, N_2, M_2}[u_{\text{DNN},\#}] + \frac{1}{2}\varepsilon \leq \frac{1}{2}(A + \varepsilon) \leq A, \\ \|u_\#\|_{L_t^p W_x^{1,q}(I \times \mathbb{R})} &\leq \mathcal{J}_{p, q, N_3, M_3}[u_{\text{DNN},\#}] + \frac{1}{2}\varepsilon \leq \frac{1}{2}(B + \varepsilon) \leq B. \end{aligned}$$

Additionally, using again the Hypothesis (H1),

$$\begin{aligned} \|\mathcal{E}[u_\#]\|_{L_t^{p'} W_x^{1,q'}(I \times \mathbb{R})} &\leq \mathcal{J}_{p', q', N_4, M_4}[\mathcal{E}[u_{\text{DNN},\#}]] + \frac{1}{2}\varepsilon \leq \frac{1}{2}\varepsilon + \frac{1}{2}\varepsilon = \varepsilon, \\ \|e^{it\partial_x^2}(u_0 - u_\#(0))\|_{L_t^p W_x^{1,q}(I \times \mathbb{R})} &\leq \mathcal{J}_{p, q, N_5, M_5}[e^{it\partial_x^2}(u_0 - u_{\text{DNN},\#}(0))] + \frac{1}{2}\varepsilon \leq \frac{1}{2}\varepsilon + \frac{1}{2}\varepsilon = \varepsilon. \end{aligned}$$

The hypotheses (4.1)-(4.5) in Lemma 4.1 are satisfied and one has that there exists a solution  $u \in \mathcal{S}'(I \times \mathbb{R})$  to (1.1) on  $I \times \mathbb{R}$  with initial data  $u_0 \in H^1(\mathbb{R})$  such that

$$\begin{aligned} \|u - u_{\#}\|_{L_t^p W_x^{1,q}(I \times \mathbb{R})} &\leq C(A, \tilde{A}, B)\varepsilon, \\ \|u - u_{\#}\|_{\mathcal{S}'(I \times \mathbb{R})} &\leq C(A, \tilde{A}, B), \\ \|u - u_{\#}\|_{L_t^{\infty} H_x^1(I \times \mathbb{R})} &\leq C(A, \tilde{A}, B). \end{aligned}$$

The final conclusion (1.3)-(1.4)-(1.5) are obtained after considering the subinterval  $[-R, R]$  and recalling that  $u_{\#} = u_{\text{DNN},\#}$  in this interval.

## 6. NUMERICAL RESULTS

**6.1. Application to Solitary waves.** Theorem 1.1 provides a first rigorous setting for the approximation of NLS solitons. Indeed, solitary waves are essential features of focusing NLS [Caz03]. In the case  $\alpha = 3$ , NLS is integrable and one has solitons, multisolitons and breathers. See e.g. [Caz03, Caz89, AFM21, AFM20, AC24, SY74] for a detailed literature. For further reading about breather solutions in other models see [Wad73, AM13, BMW94, AMP17].

**Corollary 6.1.** *Let  $\alpha \in [2, 5)$  and  $\varepsilon > 0$ . Let  $u(t) \in H^1(\mathbb{R})$  be any NLS solitary wave solution; or soliton, multi-soliton or breather if  $\alpha = 3$ . Then there is  $\tilde{A} = \tilde{A}(\varepsilon, I) = o_{\varepsilon}(1)$ , such that the following holds. Assume that  $u_{\text{DNN},\#}$  is a DNN-generated realization of a PINNs  $\Phi$  such that (H1)-(H3) are satisfied with  $\tilde{A}$  as above. Then for all  $R > 0$  sufficiently large,*

$$\|u - u_{\text{DNN},\#}\|_{L_t^{\infty} H_x^1(I \times [-R, R])} \lesssim_{A,B} \varepsilon.$$

The proof of this fact follows immediately from Remark 3.1 and the continuity of the flow. It is an open question to introduce and mix standard stability techniques in the description of PDEs via PINNs. Although Corollary 6.1 may be considered as a consequence of the continuity of the flow, we will argue below that numerical tests corroborate Theorem 1.1 and the “long time stability” nature of the approximate PINNs solutions.

**6.2. Numerical tests. Preliminaries.** We have performed numerical tests to validate Theorem 1.1 and Corollary 6.1 in the special case of well-recognized NLS solitary waves. All the simulations have been performed in Python on a 64-bit MacBook Pro M2 (2022) with 8GB of RAM.

First of all, we have chosen  $\alpha = 3$  which is the integrable case. In this situation, numerous explicit solitons are available. In this case,  $(p, q) = (8, 4)$ , and  $p' = \frac{8}{7}$  and  $q' = \frac{4}{3}$  are the Hölder conjugates of  $p$  and  $q$ , respectively. We aim to obtain numerically an approximation  $u_{\text{DNN},\#}$  by performing an algorithm in Python. The full details of the implemented algorithm are the following:

- (i) We start with a DNN  $u_{\text{DNN},\#} := u_{\text{DNN},\#\theta}$  having 4 hidden layers, 20 neurons per layer and the classical sine activation function acting component-wise. The weights and biases will be initialized in a standard way, using the Glorot uniform initializer. They will be summarized in  $\theta$  as the optimization variables.
- (ii) To optimize the DNN parameters, we will use the LBFGS method (see, e.g. [Fle13, KoWh19]), which in our case performed better than the standard Adam method, with 3000 iterations.
- (iii) For  $N_4, M_4, N_5, M_5$  as in (H3) we choose the points  $(x_{4,j})_{j=1}^{N_4}, (x_{5,j})_{j=1}^{N_5} \subset [-R, R]$ , and  $(t_{4,\ell})_{\ell=1}^{M_4}, (t_{5,\ell})_{\ell=1}^{M_5} \subset [-T, T]$  to obtain two grids of  $M_4 \times N_4$  and  $M_5 \times N_5$  points  $(t_{4,\ell}, x_{4,j})_{\ell,j=1}^{M_4, N_4}$  and  $(t_{5,\ell}, x_{5,j})_{\ell,j=1}^{M_5, N_5}$ , respectively.

Unless we say the opposite, we will take in the numerical simulations  $N_4 = N_5 = M_4 = M_5 = 32$ , and  $(x_{4,j})_{j=1}^{N_4} = (x_{5,j})_{j=1}^{N_5}$ ,  $(t_{4,\ell})_{\ell=1}^{M_4} = (t_{5,\ell})_{\ell=1}^{M_5}$  will be taken as uniformly partitions over  $[-R, R]$  and  $[-T, T]$ , respectively.

- (iv) We will consider the loss function as the functions defined in (H3): First, for simplicity define

$$v(t, \cdot) \equiv e^{it\partial_x^2}(u_0 - u_{\text{DNN},\#}(0)).$$

As said before, this linear evolution can be computed using an approximation on the corresponding Fourier transform. Denote as  $\hat{v}(t_{\ell}, x_j)$  the approximation of  $v$  at the point  $(t_{\ell}, x_j)$ . Then the loss

function takes the form:

$$\begin{aligned} \text{Loss}(\theta) &:= \mathcal{J}_{p',q',N_4,M_4}[\mathcal{E}[u_{\text{DNN},\#}]] + \mathcal{J}_{p,q,N_5,M_5}[\hat{v}] \\ &= \left( \frac{1}{M_4} \sum_{\ell=1}^{M_4} \left( \frac{1}{N_4} \sum_{j=1}^{N_4} |\mathcal{E}[u_{\text{DNN},\#}](\hat{t}_\ell, \hat{x}_j)|^{q'} \right)^{\frac{p'}{q'}} \right)^{\frac{1}{p'}} + \left( \frac{1}{M_5} \sum_{\ell=1}^{M_5} \left( \frac{1}{N_5} \sum_{j=1}^{N_5} |\hat{v}(t_\ell, x_j)|^q \right)^{\frac{p}{q}} \right)^{\frac{1}{p}}, \end{aligned} \quad (6.1)$$

where we recall  $\mathcal{E}[u_{\text{DNN},\#}] := i\partial_t u_{\text{DNN},\#} + \partial_x^2 u_{\text{DNN},\#} + |u_{\text{DNN},\#}|^{\alpha-1} u_{\text{DNN},\#}$ .

(v) In each example we aim to obtain numeric values for the bounds involved in (H2). For this, along this section we consider in each iteration step the quantities

$$\tilde{A} := \mathcal{J}_{H^1,N_1}[u_0 - u_{\text{DNN},\#}(0)],$$

$$A := \mathcal{J}_{\infty,H^1,N_2,M_2}[u_{\text{DNN},\#}], \quad B := \mathcal{J}_{p,q,N_3,M_3}[u_{\text{DNN},\#}],$$

where  $u_{\text{DNN},\#}$  is the respective DNN of each iteration in the LBFGS algorithm and  $N_1 = N_2 = N_3 = N_5$  and  $M_2 = M_3 = M_5$ .

(vi) Consider  $N_{\text{test}} = M_{\text{test}} = 100$ . We will use as test data a grid of  $N_{\text{test}} \times M_{\text{test}}$  points  $(t_\ell, x_j)_{\ell,j=1}^{M_{\text{test}},N_{\text{test}}}$  generated in the same way as the training points. If  $u = u(t, x)$  is the exact solution of the NLS equation, we will compute the following errors

$$\text{error}_{\mathcal{S}'} := \max_{(p,q)} \mathcal{J}_{p,q,N_{\text{test}},M_{\text{test}}}[u_{\text{DNN},\#} - u], \quad (6.2)$$

$$\text{error}_{L_t^p W_x^{1,q}} := \mathcal{J}_{p,q,N_{\text{test}},M_{\text{test}}}[u_{\text{DNN},\#} - u], \quad (6.3)$$

$$\text{error}_{L_t^\infty H^1} := \mathcal{J}_{\infty,H^1,N_{\text{test}},M_{\text{test}}}[u_{\text{DNN},\#} - u], \quad (6.4)$$

where in (6.2) we take the maximum over a suitable grid of values of  $q$  that makes the pair  $(p, q)$  Schrödinger admissible and  $(p, q) = (8, 4)$  in (6.3).

*Remark 6.1* (On the approximation of  $v(t, \cdot)$ ). Recall that  $v(t, \cdot)$  is given by

$$\mathcal{F}_{\xi \rightarrow x}^{-1} \left( e^{-it\xi^2} \mathcal{F}_{x \rightarrow \xi}(u_0 - u_{\text{DNN},\#}(0))(\xi) \right).$$

We will approximate  $v(t_\ell, x_j)$  by using the `fft` package in Pytorch, that uses the fast Fourier transform (FFT) to obtain a numerical approximation of the (continuous) Fourier transform  $\mathcal{F}_{x \rightarrow \xi}$ . Thus the value of  $\hat{v}(t_\ell, x_j)$  is obtained as follows:

- (1) Generate an uniform grid of 100 points in  $[-R, R]$ . For each point  $x_k$  in the grid compute the FFT of  $u_0(x_k) - u_{\text{DNN},\#}(0, x_k)$ .
- (2) Generate the frequencies  $\xi_k$  related to each  $x_k$ .
- (3) Obtain  $\hat{v}(t_\ell, x_j)$  from the following mean

$$\hat{v}(t_\ell, x_j) = \frac{1}{100} \sum_{k=1}^{100} e^{-it\xi_k^2} \text{FFT}[u_0(x_k) - u_{\text{DNN},\#}(0, x_k)] e^{i\xi_k x_j}.$$

**6.3. List of solitary waves.** Following [AFM21], let  $c, \nu > 0$  be fixed scaling parameters. The considered solutions will be: the solitary wave

$$Q(t, x) = e^{i\frac{\nu}{2}x - i\left(\frac{\nu^2}{4} - c\right)t} \sqrt{2c} \operatorname{sech}(\sqrt{c}(x - \nu t)). \quad (6.5)$$

(notice that if  $\nu = 0$ , then the solitary-wave solution remains to a standing wave solution), the Peregrine breather [Per83]

$$B_{\text{P}}(t, x) := e^{it} \left( 1 - \frac{4(1+2it)}{1+4t^2+2x^2} \right), \quad (6.6)$$

and the Kuznetsov-Ma breather [Kuz77, Ma79]

$$B_{\text{KM}}(t, x) := e^{it} \left( 1 - \sqrt{2}\tilde{\beta} \frac{\tilde{\beta}^2 \cos(\tilde{\alpha}t) + i\tilde{\alpha} \sin(\tilde{\alpha}t)}{\tilde{\alpha} \cosh(\tilde{\beta}x) - \sqrt{2}\tilde{\beta} \cos(\tilde{\alpha}t)} \right), \quad (6.7)$$

with

$$\tilde{\alpha} := (8a(2a-1))^{\frac{1}{2}}, \quad \tilde{\beta} := (2(2a-1))^{\frac{1}{2}}, \quad a > \frac{1}{2},$$

Notice that the Kuznetsov-Ma breather does not converge to zero at infinity, but after the subtraction of the background, it becomes a localized solution. Additionally, if  $\alpha \in (1, 5)$ ,  $\alpha \neq 3$ , and  $\omega > 0$ , we shall consider the standing wave solution

$$u_\omega(t, x) = e^{i\omega t} \left( \left( \frac{\alpha+1}{2} \right) \omega \operatorname{sech}^2 \left( \frac{\alpha-1}{2} \sqrt{\omega} x \right) \right)^{\frac{1}{\alpha-1}}. \quad (6.8)$$

We have chosen  $N = 100$  and  $M = 100$  in every error computation, representing a grid of  $10^4$  space-time evaluation points. The training data will be the exact soliton or solitary wave solution evaluated at  $32 \times 32$  points for each member in (6.1).

**6.4. Solitons.** We present now our first results for the case of the soliton  $Q$  in (6.5). We choose parameters  $c = \nu = 1$  but we ensure that our results are very similar for other similar values of  $c$  and  $\nu$ . The space region is  $[-8, 8]$  and the time region  $[-2, 2]$ . Our results are summarized in Fig. 1, where the continuous line represents the exact solution and the dashed line is the solution computed using the proposed PINNs minimization procedure. In particular, Fig. 1a and 1b present respectively the real and imaginary parts of the computed soliton solution for three different times.

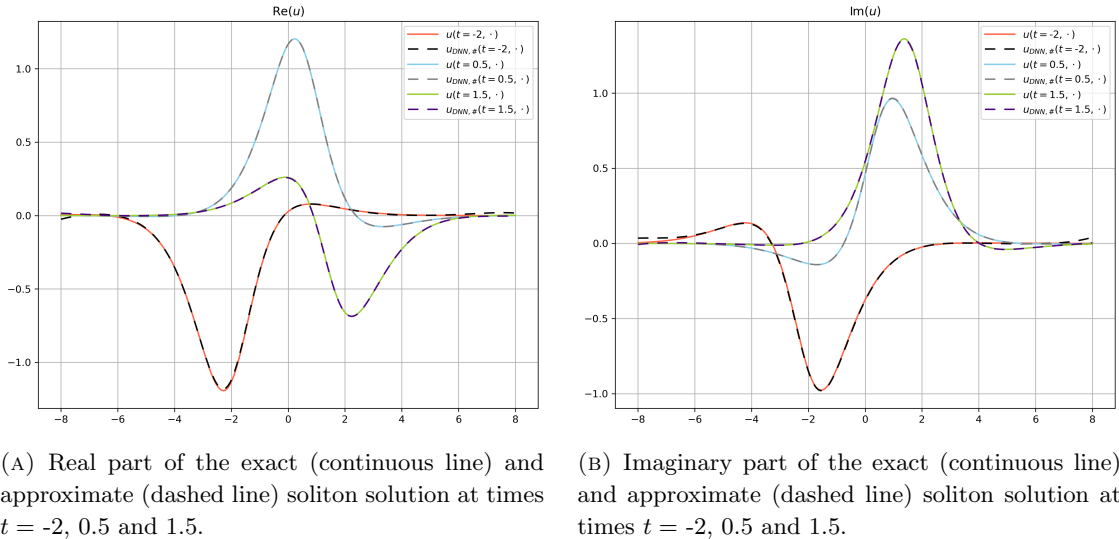


FIGURE 1. Approximation of the soliton solution in the case  $c = \nu = 1$ .

In Fig. 2, the evolution of the computed constants  $\tilde{A}$ ,  $A$ ,  $B$ , and the error of the approximation is presented in terms of the number of iterations of the numerical algorithm for the soliton solution with values  $\alpha = \beta = 1$ . It is noticed in Fig. 2a that the constant  $\tilde{A}$ , measuring the  $H^1$  difference between the approximate solution at time zero and the initial data decreases in time, revealing that to get a better approximation for all posterior times, it is necessary to get very small errors at the initial time. Concerning the evolution of the computed values for the constants  $A$  and  $B$ , graphed in Figs. 2b and 2c, despite certain “explosions” produced during the evolution of the algorithm, they stabilize at some  $O(1)$  value during a big part of the numerical procedure. The error function (6.1), graphed in Fig. 2d, naturally decreases through computations to achieve an  $O(10^{-3})$  value.

Table 1 summarizes the elapsed time and the evolution through the iterations of the associated norms of the difference between the exact and the approximate solutions in the case of the soliton with values  $c = \nu = 1$ . The time interval in these cases is  $[-2, 2]$ , and the space interval is  $[-8, 8]$ . These norms are computed using (6.2), (6.3) and (6.4) with uniform weights equal 1, and uniform  $N_{\text{test}}$  and  $M_{\text{test}}$  given by 100. As a conclusion, from Table 1 we deduce that, during the numerical computations all the norms involved in Theorem 1.1 decreased to a value of order  $10^{-2}$  and it takes less than one minute.

Fig. 3 computes the  $L_t^p W_x^{1,q}$  error (6.3) of the trained DNN  $u_{\text{DNN},\#}$  for different admissible pairs  $(p, q)$ . The values of  $q$  are chosen uniformly as a grid of 197 points between 2 and 100, namely,  $q = \frac{k}{2}$  for  $k = 4, \dots, 200$ . Our numerical simulations suggest that for large values of  $q$ , error  $L_t^p W_x^{1,q}$  is zero, and that the worst case of error  $\mathcal{S}'$  in the trained DNN was dictated by the  $L_t^\infty H_x^1$  norm or values close to it.

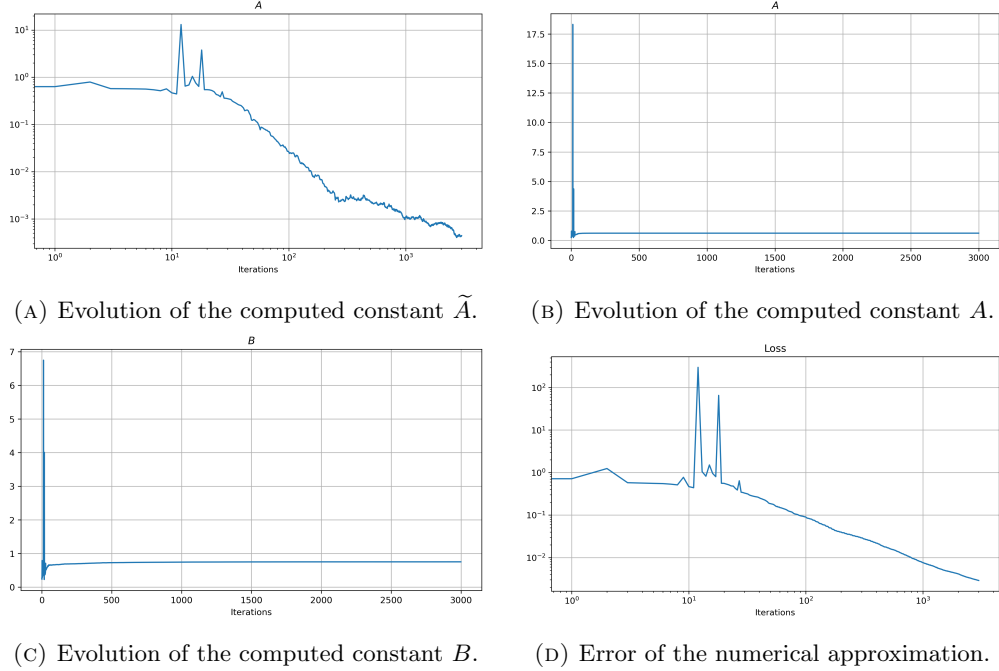


FIGURE 2. Evolution of the constants  $\tilde{A}$ ,  $A$  and  $B$  and the error (6.1) during the optimization algorithm.

Iterations	Elapsed time [s]	error $L_t^p W_x^{1,q}$	error $L_t^\infty H^1$	error $\mathcal{S}'$
100	1.846	0.434	0.515	0.668
500	9.436	0.128	0.162	0.186
1000	18.654	$6.268 \times 10^{-2}$	$8.161 \times 10^{-2}$	$8.691 \times 10^{-2}$
3000	57.791	$1.308 \times 10^{-2}$	$2.051 \times 10^{-2}$	$2.051 \times 10^{-2}$

TABLE 1. Computed values of the elapsed time and norms involved in Theorem 1.1, for five different number of iterations in the solitonic case.

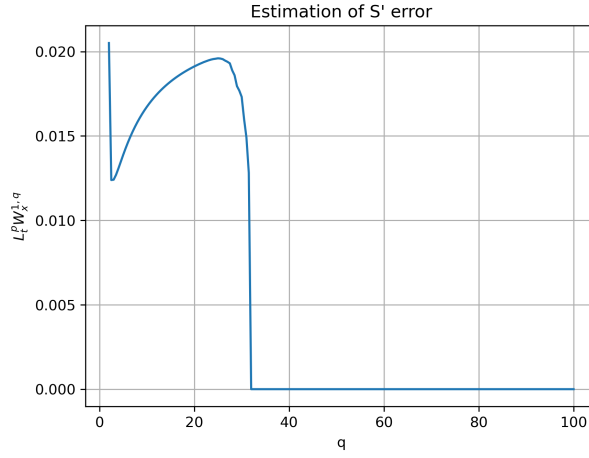


FIGURE 3.  $L_t^p W_x^{1,q}$  error for different admissible pairs  $(p, q)$  in the solitonic case. The x-axis represents 100 points of  $q$  uniformly chosen between 2 and 50, and the y-axis represents the  $L_t^p W_x^{1,q}$  error, where  $p = \frac{4q}{q-2}$ . The  $\mathcal{S}'$  error will be computed as the maximum of the  $L_t^p W_x^{1,q}$  error in the grid of  $q$ .

**6.5. Kuznetsov-Ma.** Even if this breather solution is not in Sobolev spaces, one can perform a similar analysis since Theorem 1.1 only consider the difference of solutions. In the case of the KM breather  $B_{\text{KM}}$

described in (6.7), we have chosen the parameter  $a = \frac{3}{4}$ . Notice that the larger is  $a$ , the more complicated are numerical simulations. In this case, the space region is  $[-5, 5]$ , and the time region  $[-1, 1]$ . Our results are summarized in Fig. 4, where the continuous line represents the exact solution and the dashed line is the solution computed using the proposed PINNs minimization procedure. In particular, Fig. 4a and 4b present respectively the real and imaginary parts of the computed breather solution for three different times.

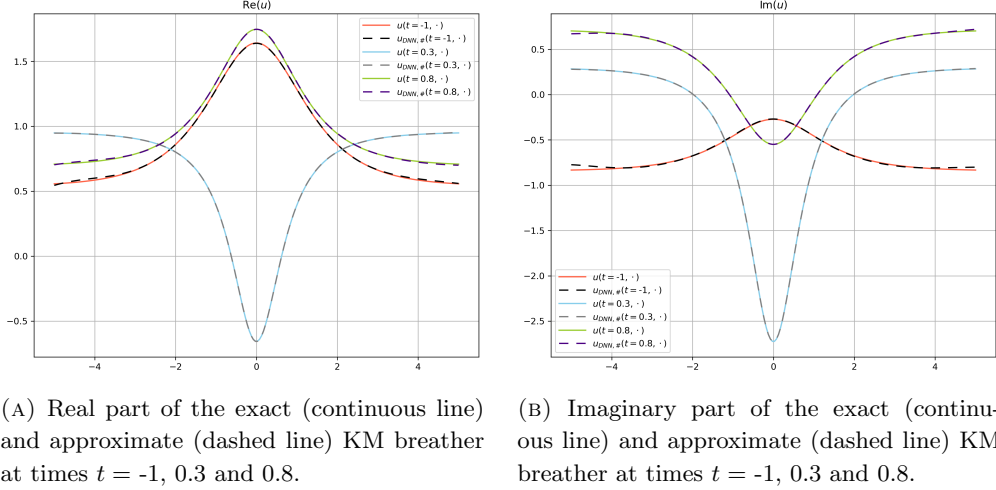


FIGURE 4. Exact (continuous line) and approximate (dashed line) KM breather at times  $t = -1, 0.3$  and  $0.8$ .

In Fig. 5, the evolution of the computed constants  $\tilde{A}$ ,  $A$ ,  $B$ , and the error of the approximation is presented in terms of the number of iterations of the numerical algorithm for the KM solution. In this case Figs. 5a-5b-5c and 5d are in agreement with the description already found in the soliton case, with the difference that in the KM breather case there are not “explosions” in the evolution of the algorithm for  $\tilde{A}$ ,  $A$ ,  $B$  and the optimization loss.

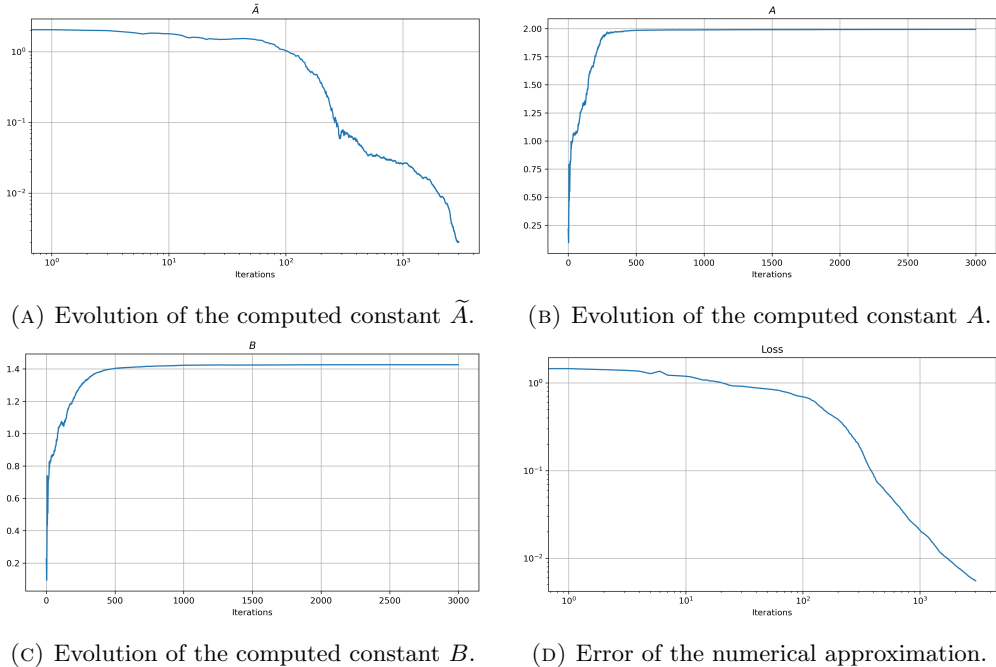


FIGURE 5. Computed evolution of the error and constants  $\tilde{A}$ ,  $A$  and  $B$  in the case of the KM breather.

Table 2 summarizes the elapsed time and the evolution through the iterations of the associated norms of the difference between the exact and the approximate solutions in the case of the KM breather with  $a = \frac{3}{4}$ . The time interval in these cases is  $[-1, 1]$ , and the space interval is  $[-5, 5]$ . These norms are computed using (6.2), (6.3) and (6.4) with uniform weights equal 1, and uniform  $N_{\text{test}}$  and  $M_{\text{test}}$  given by 100. As a conclusion, from Table 2 we deduce that, during the numerical computations all the norms involved in Theorem 1.1 decreased to a value of order  $10^{-2}$  and it takes less than one minute.

Iterations	Elapsed time [s]	error $L_t^p W_x^{1,q}$	error $L_t^\infty H^1$	error $S'$
100	1.823	1.649	1.669	2.560
500	9.487	0.226	0.307	0.323
1000	18.840	$3.832 \times 10^{-2}$	$7.079 \times 10^{-2}$	$9.946 \times 10^{-2}$
3000	59.416	$1.726 \times 10^{-2}$	$2.922 \times 10^{-2}$	$2.922 \times 10^{-2}$

TABLE 2. Computed values of the elapsed time and norms involved in Theorem 1.1, for five different number of iterations in the KM breather case.

Later, in Table 3, we present the values of computation time, loss function (6.1), computed approximate values for  $\tilde{A}$ ,  $A$ ,  $B$ , and the approximate norms  $L_t^p W_x^{1,q}$ ,  $L_t^\infty H_x^1$  and  $S'$  for the whole space-time computation. This is done for four different values of  $a$ . For this we fix  $[-4, 4]$  the space region,  $[-0.5, 0.5]$  the time region and 40 neurons per hidden layer. It is noticed that errors are usually of the order  $10^{-2}$ . Then, the constant  $\tilde{A}$  is usually found small of the order  $10^{-3}$ , as one might expect when approximating the solution for all times. but the norms  $A$  and  $B$  are reasonably bounded below 4. Finally, the three computed norms involved in Theorem 1.1 are suitably small, but two order higher than the value of  $\tilde{A}$ , and the  $S'$  norm is dictated by the  $L_t^\infty H^1$  norm.

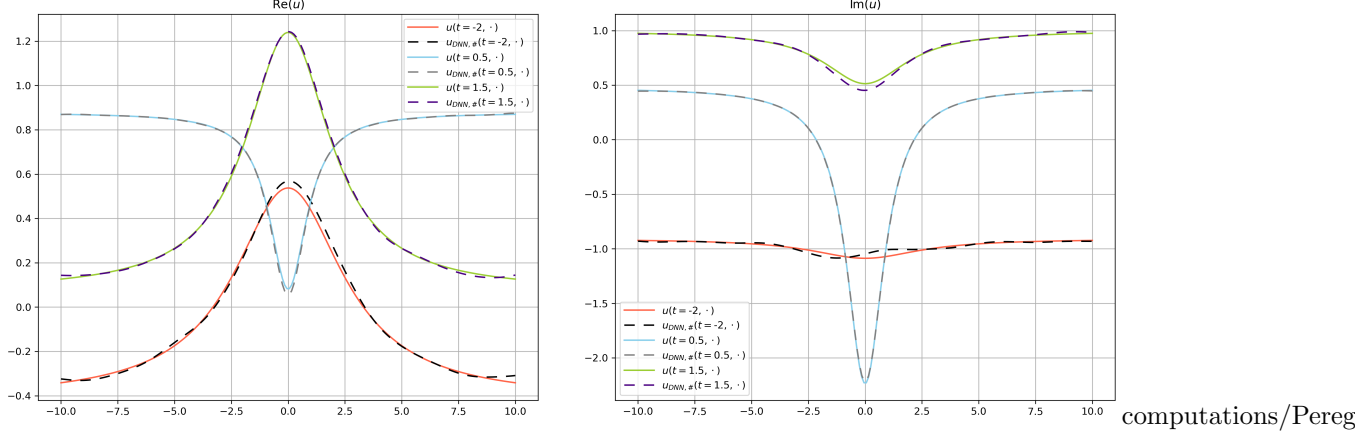
	$a = 3/4$	$a = 1$	$a = 3/2$	$a = 2$
Elapsed Time [s]	92.791	87.610	102.096	100.890
Loss	$3.605 \times 10^{-3}$	$4.358 \times 10^{-3}$	$6.588 \times 10^{-3}$	$1.184 \times 10^{-2}$
$\tilde{A}$	$3.466 \times 10^{-3}$	$6.158 \times 10^{-3}$	$2.024 \times 10^{-3}$	$4.184 \times 10^{-3}$
$A$	2.175	2.459	2.955	3.403
$B$	1.589	1.690	1.851	1.987
$L_t^p W_x^{1,q}$	$8.691 \times 10^{-3}$	$1.055 \times 10^{-2}$	$9.202 \times 10^{-3}$	$2.012 \times 10^{-2}$
$L_t^\infty H_x^1$	$1.848 \times 10^{-2}$	$2.366 \times 10^{-2}$	$2.112 \times 10^{-2}$	$4.736 \times 10^{-2}$
$S'$	$1.848 \times 10^{-2}$	$2.366 \times 10^{-2}$	$2.112 \times 10^{-2}$	$4.736 \times 10^{-2}$

TABLE 3. Computed values of the elapsed time, errors, constants and norms involved in Theorem 1.1, for four different values of  $a$ , in the KM breather case.

**6.6. Peregrine breather.** This is also another example of a solution with nonzero background at infinity for which the numerical approach works in a satisfactory fashion. We consider the case of the Peregrine breather  $B_P$  described in (6.6). Note that in this case there is no extra parameter that builds a family of solutions of the form of (6.6). As before, the space region is  $[-10, 10]$  and the time region  $[-2, 2]$ . However, in this case we choose  $N_4 = M_4 = 64$  and  $N_5 = M_5 = 32$ . Our results are summarized in Fig. 6, where the continuous line represents the exact solution and the dashed line is the solution computed using the proposed PINNs minimization procedure. In particular, Fig. 6a and 6b present respectively the real and imaginary parts of the computed breather solution for three different times.

In Fig. 7, the evolution of the computed constants  $\tilde{A}$ ,  $A$ ,  $B$ , and the error of the approximation is presented in terms of the number of iterations of the numerical algorithm for the Peregrine solution. Figs. 7a-7b-7c and 7d are in agreement with the description already found in the previous cases.

Table 4 summarizes the elapsed time and the evolution through the iterations of the associated norms of the difference between the exact and the approximate solutions in the case of the Peregrine breather. The time interval in these cases is  $[-2, 2]$ , and the space interval is  $[-10, 10]$ . These norms are computed using (6.2), (6.3) and (6.4) with uniform weights equal 1, and uniform  $N_{\text{test}}$  and  $M_{\text{test}}$  given by 100. As



(A) Real part of the exact (continuous line) and approximate (dashed line) Peregrine breather at times  $t = -2, 0.5$  and  $1.5$ .

(B) Imaginary part of the exact (continuous line) and approximate (dashed line) Peregrine breather at times  $t = -2, 0.5$  and  $1.5$ .

FIGURE 6. Exact (continuous line) and approximate (dashed line) Peregrine breather at times  $t = -2, 0.5$  and  $1.5$ .

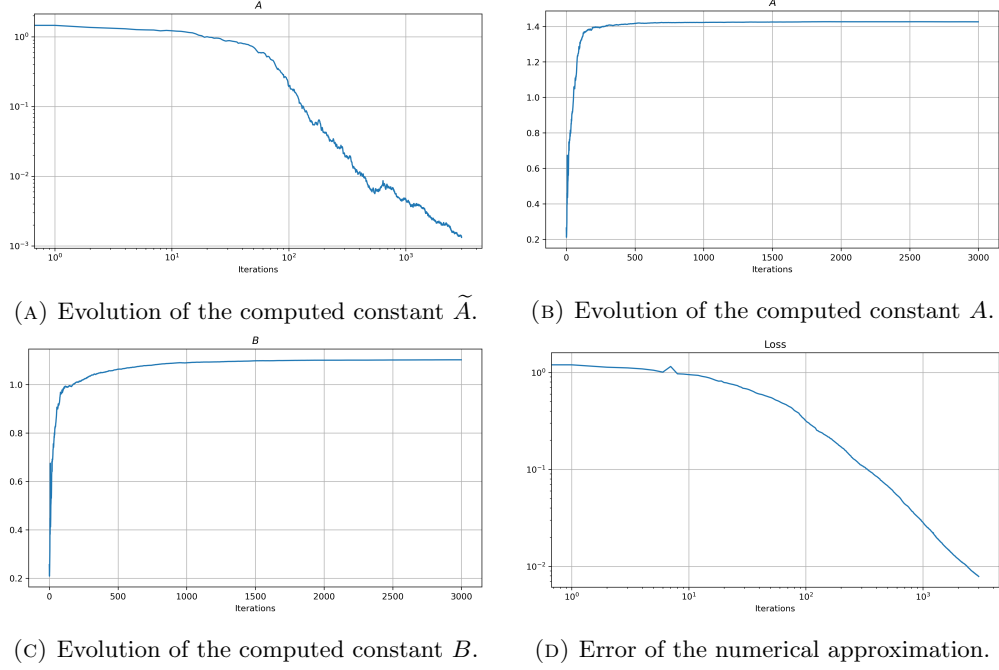


FIGURE 7. Computed evolution of the error and constants  $\tilde{A}$ ,  $A$  and  $B$  in the case of the Peregrine breather.

a conclusion, from Table 4 we deduce that, during the numerical computations all the norms involved in Theorem 1.1 decreased to a value of order  $10^{-2}$  and it takes around 1 minute 20 seconds. Note in this case the convergence is slower than in the previous solitonic and KM breather cases.

**6.7. Sensitivity analysis.** We will now focus in the solitonic case and by previous experiment we are hoping that these results are similar to the breather cases.

First of all we study the variation on the hyperparameters of the solution. In particular, Tables 5 and 6 present the values of computation time, loss function (6.1), computed approximate values for  $\tilde{A}$ ,  $A$ ,  $B$ , and the approximate norms  $L_t^p W_x^{1,q}$  and  $L_t^\infty H^1$  for the whole space-time computation. This is done for two and three different values of  $c$  and  $\nu$ , respectively. For this we fix  $[-8, 8]$  the space region and  $[-1, 1]$

Iterations	Elapsed time [s]	error <sub><math>L_t^p W_x^{1,q}</math></sub>	error <sub><math>L_t^\infty H^1</math></sub>	error <sub><math>S'</math></sub>
100	3.987	1.128	1.140	1.761
500	21.083	0.601	0.618	0.896
1000	42.992	0.222	0.242	0.330
3000	140.311	$3.257 \times 10^{-2}$	$4.154 \times 10^{-2}$	$4.753 \times 10^{-2}$

TABLE 4. Computed values of the elapsed time and norms involved in Theorem 1.1, for five different number of iterations in the Peregrine breather case.

$\nu$	1	3	5
Elapsed Time [s]	60.066	59.385	58.422
Loss	$2.261 \times 10^{-3}$	$1.756 \times 10^{-3}$	$4.127 \times 10^{-3}$
$\tilde{A}$	$3.753 \times 10^{-4}$	$5.918 \times 10^{-4}$	$8.153 \times 10^{-4}$
$A$	0.619	0.932	1.356
$B$	0.753	0.754	0.754
error <sub><math>L_t^p W_x^{1,q}</math></sub>	$3.959 \times 10^{-3}$	$5.308 \times 10^{-3}$	$7.199 \times 10^{-3}$
error <sub><math>L_t^\infty H^1</math></sub>	$5.752 \times 10^{-3}$	$7.775 \times 10^{-3}$	$1.632 \times 10^{-2}$
error' <sub><math>S</math></sub>	$6.717 \times 10^{-3}$	$8.937 \times 10^{-3}$	$1.632 \times 10^{-2}$

TABLE 5. Computed values of the elapsed time, errors, constants and norms involved in Theorem 1.1, for  $c = 1$  and three different values of  $\nu$ , in the solitonic case.

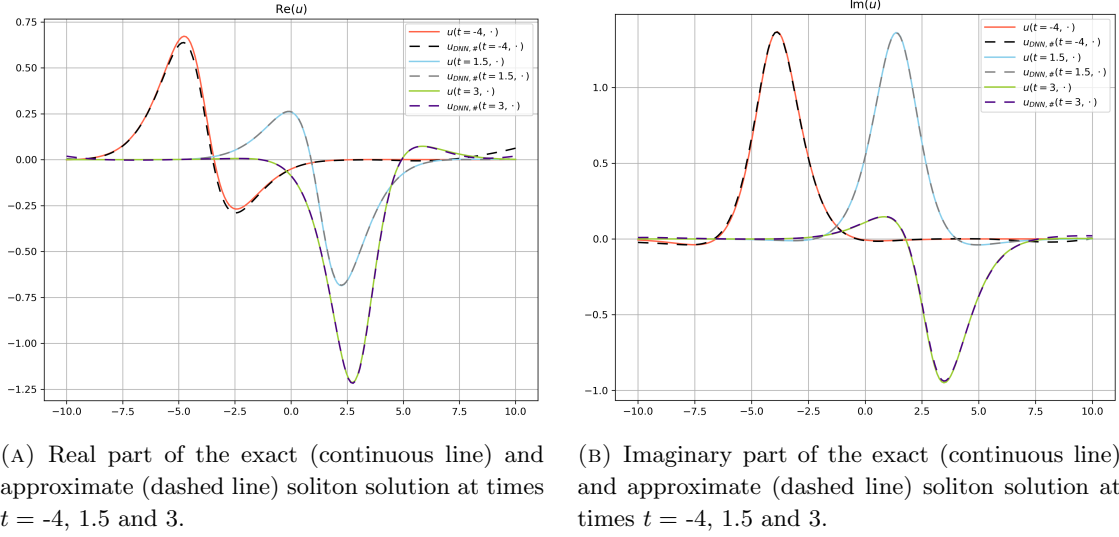
$\nu$	1	3	5
Elapsed Time [s]	60.066	57.748	60.053
Loss	$4.388 \times 10^{-3}$	$6.329 \times 10^{-3}$	$5.289 \times 10^{-3}$
$\tilde{A}$	$7.035 \times 10^{-4}$	$9.144 \times 10^{-4}$	$8.482 \times 10^{-4}$
$A$	0.975	1.337	1.861
$B$	1.136	1.136	1.138
error <sub><math>L_t^p W_x^{1,q}</math></sub>	$1.887 \times 10^{-2}$	$1.774 \times 10^{-2}$	$1.918 \times 10^{-3}$
error <sub><math>L_t^\infty H^1</math></sub>	$2.661 \times 10^{-2}$	$2.823 \times 10^{-2}$	$4.649 \times 10^{-3}$
error' <sub><math>S</math></sub>	$2.838 \times 10^{-2}$	$2.823 \times 10^{-2}$	$4.649 \times 10^{-3}$

TABLE 6. Computed values of the elapsed time, errors, constants and norms involved in Theorem 1.1, for  $c = 3$  and three different values of  $\nu$ , in the solitonic case.

the time region. It is noticed that errors are usually of the order  $10^{-2}$ . Then, the constant  $\tilde{A}$  is usually found small, as one might expect when approximating the solution for all times. but the norms  $A$  and  $B$  are reasonably bounded below 2,  $A$  increases when  $\nu$  increases and  $B$  almost does not change for fixed  $c$  and variable  $\nu$ . Finally, the three computed norms involved in Theorem 1.1 are suitably small, but one or two orders higher than the value of  $\tilde{A}$ .

**Effect of time:** In order to study the performance of the algorithm, we will change the size of the time interval. For this aim, we consider 5000 iterations, 40 neurons per hidden layer  $N_4 = 128$  and  $N_5 = M_4 = M_5 = 32$ . Fig. 8 summarizes the performance of the solitonic case with  $c = \nu = 1$  in the space region  $[-10, 10]$  and the time region  $[-4, 4]$ , where the continuous line represents the exact solution and the dashed line is the solution computed using the proposed PINNs minimization procedure. In particular, Fig. 8a and 8b present respectively the real and imaginary parts of the computed soliton solution for three different times. Our simulations suggest that for greater values of the time interval, the train grid needs to be fine-tuned.

In this case the algorithm takes 227.659 seconds, and obtaining errors  $\text{error}_{L_t^p W_x^{1,q}} = 2.081 \times 10^{-2}$ ,  $\text{error}_{L_t^\infty H^1} = 2.739 \times 10^{-2}$ ,  $\text{error}_S = 3.051 \times 10^{-2}$ , loss =  $1.453 \times 10^{-3}$  with constants  $\tilde{A} = 1.654 \times 10^{-4}$ ,  $A = 0.561$  and  $B = 0.715$ .

FIGURE 8. Approximation of the soliton solution in the case  $c = \nu = 1$ .

## 7. DISCUSSIONS AND CONCLUSIONS

**7.1. Discussion.** Currently, PINN methodology has been successfully applied for solving analytically and numerically various NLS equations in bounded domains, by combining underlying physics laws and neural networks to obtain precise solutions with minimal data [SSH22, BKM22, HaDe23, PLC21, WaYa21, ZhBa22, BMAR23, RPP19, Rai18, TSVS24]. All these works are focused to limited spatial domains, which do not describe current physical phenomena appearing in nature associated with slow spatial decay solutions (or long-ranged potentials). In the case of unbounded spatial domain, recent advances have been presented in the last years: in [XCL21], a DNN was implemented to construct the so called *absorbing boundary condition* (ABC), which confines the computation to a finite domain, and an ABC is then imposed on the boundary to minimize undesirable reflections. Instead, simply removing the exterior (unbounded) region, the ABC provides an efficient approach to replicate the influence from the surrounding environment. This approach was tested with the wave and the Schrödinger equations posed in unbounded domains. In [FWP23], they realized that PINNs, despite their power and wide use, are generally known for being hard to train and may give rise to several practical pathologies, like the ones which arise in the numerical solution of acoustic wave scattering problems [Colt98]. Such scattering problems are usually posed in unbounded domains, rendering most existing PINNs formulations infeasible, due to their need to sample collocation points in an infinite domain. In [FWP23] they used the so called, *boundary integral equations* (BIEs) which are a well-established method for solving PDEs, particularly for problems with complex geometries or unbounded domains. In fact, BIEs allow to represent the solution of a PDE in terms of its boundary values, and can be solved using various techniques. See [WWLL23] for a similar approach.

Finally, [XBC23] dealt with unbounded domains for the NLS equation by using a hybrid approach, combining adaptative spectral and PINN methods. This was a first step to compute the PDE evolution on unlimited regions. In fact they resorted to a few apriori assumptions on the asymptotic spatial behavior and an appropriate choice of spectral basis functions, to effectively describe the spatial dependence in terms of basis functions. In recent physical approaches, [BaEs22] dealt with the unbounded issue through introducing a similarity variable and a reasonable guess suited for estimating this new variable encompassing the infinite value or in [RRCWL24] simply truncating the computational domain to avoid unnecessary computation, and guaranteeing that the wave propagates out the computational domain without interfering with the upstream field when it passes through truncated boundaries.

In contrast, our approach dealing with unbounded domains do not resort to an external basis functions, and in fact it shows how to describe the critical focusing NLS evolution posed on the unbounded real line by introducing a condition on the evolution of the linear part and suitable approximate norms,

which under smallness assumptions when acting on certain functions, approximate NLS dynamics in a satisfactory and accurate way.

**7.2. Conclusions.** We have considered the subcritical nonlinear Schrödinger (NLS) in dimension one posed on the unbounded real line. The noncompact setting poses several important complications in approximation schemes, in particular in the case of deep neural networks, since there is no suitable restriction on the data at infinity in space. Several previous works [RPP19, BKM22] have considered from the numerical and theoretical point of view the case of NLS placed on bounded domains, providing important advances in the understanding of the approximation of dispersive solutions via DNN techniques. In this paper, we have introduced a new PINNs method based in standard physical restrictions plus a new component dealing with the linear evolution of perturbed data to treat the case of unbounded domains. We provided what we believe are the first rigorous bounds on the associated approximation error in energy and Strichartz norms, which are key in the NLS setting. This is done by assuming the reasonable condition that integration schemes are available and good enough to approximate space-time norms. Applications to traveling waves, breathers and solitons, as well as numerical experiments confirming the validity of the approximation were also provided as well, confirming that the approximation scheme works with good performance.

## REFERENCES

- [AC24] M. A. Alejo, and A. J. Corcho, *On nonexistence of NLS breathers*, arXiv:2408.09862v1 (2024).
- [AM13] M. A. Alejo, and C. Muñoz, *Nonlinear stability of mKdV breathers*. Comm. Math. Phys. 324 (1) (2013), 233–262.
- [ACM24] M. A. Alejo, L. Cossetti, L. Fanelli, C. Muñoz, and N. Valenzuela, *Bounds on the approximation error for deep neural networks applied to dispersive models: Nonlinear Schrödinger*, preprint under preparation (2024).
- [AFM21] M. A. Alejo, L. Fanelli, and C. Muñoz, *Stability and instability of breathers in the U(1) Sasa-Satsuma and nonlinear Schrödinger models*. Nonlinearity 34 (2021), no. 5, 3429–3484.
- [AFM20] M. A. Alejo, L. Fanelli, and C. Muñoz, *Review on the stability of the Peregrine and related breathers*, Frontiers in Physics, section Mathematical and Statistical Physics, Mini-Review, Front. Phys., 24 (2020).
- [AMP17] M. A. Alejo, C. Muñoz and J.M. Palacios, *On the variational structure of breather solutions I: sine-Gordon equation*. Journal of Mathematical Analysis and Applications Vol.453/2 (2017).
- [BKM22] G. Bai, U. Koley, S. Mishra, and R. Molinaro, *Physics informed Neural Networks (PINNs) for approximating nonlinear dispersive PDEs*, J. Comp. Math., 39 (2021), pp. 816–847 [10.4208/jcm.2101-m2020-0342](https://doi.org/10.4208/jcm.2101-m2020-0342).
- [BMAR23] C. Bajaj, L. McLennan, T. Andeen and A. Roy, *Recipes for when physics fails: recovering robust learning of physics informed neural networks*, Mach. Learn.: Sci. Technol. 4 (2023) 015013.
- [BaEs22] H. Bararnia and M. Esmailpour, *On the application of physics informed neural networks (PINN) to solve boundary layer thermal-fluid problems*, International Communications in Heat and Mass Transfer 132 (2022) 105890.
- [BeJe19] C. Beck and A. Jentzen. *Machine learning approximation algorithms for high-dimensional fully nonlinear partial differential equations and second-order backward stochastic differential equations*. Journal of Nonlinear Science, 29(4), 1563–1619, 2019.
- [BBGJJ21] C. Beck, S. Becker, P. Grohs, N. Jaafari and A. Jentzen. *Solving the Kolmogorov PDE by Means of Deep Learning*. Journal of Scientific Computing, vol. 88, no. 3, July 2021. <https://doi.org/10.1007/s10915-021-01590-0>.
- [BHHJK20] C. Beck, F. Hornung, M. Hutzenthaler, A. Jentzen, and T. Kruse. *Overcoming the curse of dimensionality in the numerical approximation of Allen-Cahn partial differential equations via truncated full-history recursive multilevel Picard approximations*. Journal of Numerical Mathematics, 28(4):197–222, dec 2020.
- [BHJK23] C. Beck, M. Hutzenthaler, A. Jentzen, and B. Kuckuck, *An overview on deep learning-based approximation methods for partial differential equations*. Discrete Contin. Dyn. Syst. Ser. B 28 (2023), no. 6, 3697–3746.
- [BGJ20] J. Berner, P. Grohs and A. Jentzen. *Analysis of the generalization error: Empirical risk minimization over deep artificial neural networks overcomes the curse of dimensionality in the numerical approximation of Black–Scholes partial differential equations*. SIAM J. Math. Data Science, 2(3), 631–657, 2020.
- [BMW94] B. Birnir, H.P. McKean, A. Weinstein, *The rigidity of sine-Gordon breathers*, Comm. Pure Appl. Math. 47, 1043–105, (1994).
- [BDPS24] A. Bonito, R. DeVore, G. Petrova, and J. W. Siegel, *Convergence and error control of consistent PINNs for elliptic PDEs*, arXiv:2406.09217
- [Bou99] J. Bourgain, *Global well posedness of defocusing critical nonlinear Schrödinger equation in the radial case*, Jour.AMS **12** (1999) 145–171.
- [Cas22] J. Castro. *Deep Learning schemes for parabolic nonlocal integro-differential equations*. Partial Differ. Equ. Appl. 3, no. 6, 77, 2022.
- [Cas23] J. Castro, *The Kolmogorov infinite dimensional equation in a Hilbert space via deep learning methods*. J. Math. Anal. Appl. 527 (2023), no. 2, Paper No. 127413, 40 pp.
- [CMV24] J. Castro, C. Muñoz and N. Valenzuela. *The Calderón’s problem via DeepONets*. Vietnam J. Math. 2024 (Carlos Kenig’s 70 anniversary). <https://doi.org/10.1007/s10013-023-00674-8>

[Caz89] T. Cazenave, *An introduction to Nonlinear Schrödinger equations*. Textos de Métodos Matemáticos **22**, UFRJ (1989).

[Caz03] T. Cazenave, *Semilinear Schrödinger equations*. Courant Lecture Notes in Mathematics 10. Providence, RI: (AMS); Courant Institute of Mathematical Sciences (2003).

[ChCh95] T. Chen and H. Chen. *Universal approximation to nonlinear operators by neural networks with arbitrary activation functions and its application to dynamical systems*. IEEE Transactions on Neural Networks, 6 (4): 911–917, 1995.

[Colt98] D.L. Colton and R. Kress, *Inverse acoustic and electromagnetic scattering theory*, **93**, Springer, 1998.

[RyMi22] T. De Ryck and S. Mishra. *Error Analysis for Physics-Informed Neural Networks (PINNs) Approximating Kolmogorov PDEs*. Advances in Computational Mathematics, vol. 48, no. 6, Nov. 2022. <https://doi.org/10.1007/s10444-022-09985-9>.

[RJM22] T. De Ryck, A. D. Jagtap and S. Mishra. *Error estimates for physics informed neural networks approximating the Navier-Stokes equations*. arXiv preprint arXiv:2203.09346, 2022.

[RMM24] T. De Ryck, S. Mishra, and R. Molinaro, *wPINNs: Weak Physics Informed Neural Networks for Approximating Entropy Solutions of Hyperbolic Conservation Laws*, SIAM Journal on Numerical Analysis Vol. 62, Iss. 2 (2024).

[FWP23] Z. Fang, S. Wang, P. Perdikaris, *Learning Only On Boundaries: a Physics-Informed Neural operator for Solving Parametric Partial Differential Equations in Complex Geometries*, arXiv:2308.12939

[FMR23] A. Ferrer-Sánchez, J.D. Martín-Guerrero, R. Ruiz de Austria, A. Torres-Forné and J.A. Font, *Gradient-Annihilated PINNs for Solving Riemann Problems: Application to Relativistic Hydrodynamics* arXiv:2305.08448.

[Fle13] R. Fletcher. *Practical methods of optimization*. John Wiley & Sons, (2013).

[GiVe79] J. Ginibre and G. Velo. *On the class of nonlinear Schrödinger equations I. The Cauchy problem, general case*, J. Funct. Anal. 32(1), 33-72 (1979).

[GiVe85] J. Ginibre and G. Velo. *Scattering theory in the energy space for the class of nonlinear nonlinear Schrödinger equations*, J. Math. Pures Appl. 64, 363-401 (1985).

[GoSc21] L. Gonon and C. Schwab. *Deep ReLU neural networks overcome the curse of dimensionality for partial integro-differential equations*. arXiv preprint arXiv:2102.11707, 2021.

[GrHe21] P. Grohs and L. Herrmann. *Deep neural network approximation for high-dimensional elliptic PDEs with boundary conditions*. IMA Journal of Numerical Analysis, 2021. <https://doi.org/10.1093/imanum/drab031>.

[GHJW18] P. Grohs, F. Hornung, A. Jentzen, and P. Von Wurstemberger. *A proof that artificial neural networks overcome the curse of dimensionality in the numerical approximation of Black-Scholes partial differential equations*. arXiv preprint arXiv:1809.02362, 2018.

[GRPK19] M. Gulian, M. Raissi, P. Perdikaris and G. Karniadakis. *Machine Learning of Space-Fractional Differential Equations*. SIAM Journal on Scientific Computing, vol. 41, no. 4, Jan. 2019, pp. A2485-2509. <https://doi.org/10.1137/18m1204991>.

[Had23] M.A. Haddou, *Quasi-normal modes of near-extremal black holes in dRGT massive gravity using Physics-Informed Neural Networks (PINNs)*, arXiv:2303.02395 (2023).

[HJE18] W. E. J. Han, A. Jentzen and W. E. *Solving High-Dimensional Partial Differential Equations Using Deep Learning*. Proceedings of the National Academy of Sciences, vol. 115, no. 34, Aug. 2018. <https://doi.org/10.1073/pnas.1718942115>.

[HaJe17] W. E., J. Han and A. Jentzen. *Deep learning-based numerical methods for high-dimensional parabolic partial differential equations and backward stochastic differential equations*. Commun. Math. Stat. 5(4), 349-380, 2017.

[HaDe23] L. Harcombe, Q. Den *Physics-informed neural networks for discovering localised eigenstates in disordered media*, Jour. Comp. Sci. 73 (2023) 102136.

[Hor91] K. Hornik. *Approximation Capabilities of Multilayer Feedforward Networks*, Neural Networks, Vol. 4, pp. 251-257. 1991.

[HPW20] C. Huré, H. Pham, and X. Warin. *Deep backward schemes for high-dimensional nonlinear PDEs*, Math. Comp. 89, no. 324, 1547-1579, 2020.

[HJKW20b] M Hutzenthaler, A. Jentzen, T. Kruse, T. A. Nguyen, and P. Von Wurstemberger. *Overcoming the curse of dimensionality in the numerical approximation of semilinear parabolic partial differential equations*. Proc. Royal Soc. A: Math. Phys. Eng. Sciences, 476 (2244):20190630, Dec. 2020.

[JKW23] A. Jentzen, B. Kuckuck, P. V. Wurstemberger, *Mathematical Introduction to Deep Learning: Methods, Implementations, and Theory*, preprint arXiv <https://arxiv.org/pdf/2310.20360.pdf> (2023).

[JSW21] A. Jentzen, D. Salimova, and T. Welti. *A proof that deep artificial neural networks overcome the curse of dimensionality in the numerical approximation of Kolmogorov partial differential equations with constant diffusion and nonlinear drift coefficients*. Comm. Math. Sciences, vol. 19, no. 5, 2021, pp. 1167-1205. <https://doi.org/10.4310/cms.2021.v19.n5.a1>.

[KMPT24] D. A. Kaltsas, L. Magafas, P. Papadopoulou, and G. N. Throumoulopoulos, *Multi-soliton solutions and data-driven discovery of higher-order Burgers' hierarchy equations with physics informed neural networks*, arXiv:2408.07027 (2024).

[KKLPWY21] G. E. Karniadakis, I. G. Kevrekidis, L. Lu, P. Perdikaris, S. Wang, and L. Yang, *Physics-informed machine learning*, Nature Reviews Physics, 3(6), 422-440 (2021).

[KK24] S. Kathane and S. Karagadde, *A Physics Informed Neural Network (PINN) Methodology for Coupled Moving Boundary PDEs*, arXiv:2409.10910 (2024).

[KoWh19] M. J. Kochenderfer and T. A. Wheeler. *Algorithms for Optimization*, The MIT Press, (2019).

[Kuz77] E. Kuznetsov, *Solitons in a parametrically unstable plasma*. Sov. Phys. - Dokl. **22**, p.507-8 (1977).

[Ma79] Y-C. Ma, *The perturbed plane-wave solutions of the cubic Schrödinger equation*. Stud. Appl. Math. **60**, p.43-58 (1979).

[LLF98] I. E. Lagaris, A. Likas, and D. I. Fotiadis. *Artificial neural networks for solving ordinary and partial differential equations*. IEEE Transactions on Neural Networks, 9(5):987-1000, 1998.

[LLP00] I. E. Lagaris, A. Likas, and P. G. D. *Neural-network methods for boundary value problems with irregular boundaries*. IEEE Transactions on Neural Networks, 11:1041-1049, 2000.

[LLPS93] M. Leshno, I. V. Ya. Lin, A. Pinkus, and S. Schocken, *Multilayer Feedforward Networks With a Nonpolynomial Activation Function Can Approximate Any Function*, Neural Networks, Vol. 6, pp. 861–867 (1993).

[LiPo14] F. Linares and G. Ponce, *Introduction to nonlinear dispersive equations*. Springer. 2nd ed. (2014).

[LBH15] Y. LeCun, Y. Bengio, and G. Hinton, *Deep learning*, Nature Vol. 521 28 May 2015, doi:10.1038/nature14539.

[LNPC24] N.J. Lobos, A.M. Neube, R. C. Pantig and A.S. Cornell, *Analyzing the effect of higher dimensions on the black hole silhouette, deflection angles, and PINN approximated quasinormal modes*, arXiv:2406.08078.

[LBK24] B. Lorenz, A. Bacho and G. Kutyniok. *Error Estimation for Physics-informed Neural Networks Approximating Semilinear Wave Equations*. Preprint arXiv:2402.07153 <https://arxiv.org/abs/2402.07153> (2024).

[LJK21] L. Lu, P. Jin and G. Em Karniadakis. *Learning Nonlinear Operators via DeepONet Based on the Universal Approximation Theorem of Operators*. Nature Machine Intelligence, vol. 3, no. 3, Mar. 2021. <https://doi.org/10.1038/s42256-021-00302-5>.

[LMR20] K. O. Lye, S. Mishra, and D. Ray. *Deep learning observables in computational fluid dynamics*. Journal of Computational Physics, page 109339, 2020.

[MJK20] Z. Mao, A. D. Jagtap, and G. E. Karniadakis. *Physics-informed neural networks for high-speed flows*. Computer Methods in Applied Mechanics and Engineering, 360:112789, 2020.

[MiMo20] S. Mishra, and R. Molinaro, *Estimates on the generalization error of Physics Informed Neural Networks (PINNs) for approximating a class of inverse problems for PDEs*, arXiv:2007.01138 (2020).

[MiMo22] S. Mishra, and R. Molinaro, *Estimates on the generalization error of physics-informed neural networks for approximating PDEs*, IMA Journal of Numerical Analysis (2023) Vol. 43, 1–43.

[Wad73] M. Wadati, *The Modified Korteweg-de Vries Equation*, Jour. Phys. Soc. Japan, 34, 1289-1296 (1973).

[MMN20] B. Moseley, A. Markham, and T. Nissen-Meyer. *Solving the wave equation with physics-informed deep learning*. Preprint arXiv arXiv:2006.11894, <https://arxiv.org/abs/2006.11894> (2020).

[MuVa24] C. Muñoz, and N. Valenzuela, *Bounds on the approximation error for deep neural networks applied to dispersive models: Nonlinear waves*, Preprint arXiv 2024 <https://arxiv.org/abs/2405.13566>.

[PLK19] G. Pang, L. Lu, and G. E. Karniadakis. *Fpinns: Fractional physics-informed neural networks*. SIAM Journal of Scientific Computing, 41:A2603-A2626, 2019.

[PeCh24] Wei-Qi Peng, Yong Chen, *Symmetric PINN for integrable nonlocal equations: Forward and inverse problems*, Chaos 34, 043124 (2024)

[Per83] D.H. Peregrine, *Water waves, nonlinear Schrödinger equations and their solutions*. J. Aust. Math. Soc. B 25 p.16-43, (1983).

[PLC21] J. Pu, J. Li and Y. Chen, *Solving localized wave solutions of the derivative nonlinear Schrodinger equation using an improved PINN method*, Nonlinear Dyn 105, 1723-1739 (2021).

[Rai18] M. Raissi, *Deep hidden physics models: Deep learning of nonlinear partial differential equations*. Journal of Machine Learning Research, 19(1), 932-955 (2018).

[RaKa18] M. Raissi and G. E. Karniadakis. *Hidden physics models: Machine learning of nonlinear partial differential equations*. Journal of Computational Physics, 357:125-141, 2018.

[RPK17] M. Raissi, P. Perdikaris, and G. E. Karniadakis, *Machine learning of linear differential equations using Gaussian processes*, J. Comp. Phys., 348 (2017), pp. 683-693, <https://doi.org/10.1016/j.jcp.2017.07.050>.

[RPP19] M. Raissi, P. Perdikaris, and G. E. Karniadakis. *Physics-informed neural networks: A deep learning framework for solving forward and inverse problems involving nonlinear partial differential equations*. Journal of Computational Physics, 378:686-707, 2019.

[RHS22] M. Rasht-Behesht, C. Huber, K. Shukla, G. E. Karniadakis, *Physics-informed Neural Networks (PINNs) for Wave Propagation and Full Waveform Inversions*, Jour. Geophysical Research: Solid Earth, 127, e2021JB023120. (2022).

[RRSL23] P. Ren, C. Rao, H. Sun, and Y. Liu, *Physics-informed neural network for seismic wave inversion in layered semi-infinite domain*. In arXiv:2305.05150.

[RRCWL24] P. Ren, C. Rao, S. Chen, J. X. Wang, H. Sun, Y. Liu, *SeismicNet: Physics-informed neural networks for seismic wave modeling in semi-infinite domain*, Computer Physics Communications 295 (2024) 109010.

[SZC23] S. Saqlain, W. Zhu, E. G. Charalampidis, P. G. Kevrekidis, *Discovering Governing Equations in Discrete Systems Using PINNs* Comm. Nonlin. Science and Num. Sim.126, 107498 (2023).

[SY74] J. Satsuma, and N. Yajima, *Initial Value Problems of One-Dimensional Self-Modulation of Nonlinear Waves in Dispersive Media*, Supplement of the Progress of Theoretical Physics, No. 55, 284-306, (1974).

[SSHG22] K. Shah, P. Stiller, N. Hoffmann and A. Cangi *Physics-Informed Neural Networks as Solvers for the Time-Dependent Schrödinger Equation* arXiv:2210.12522.

[TaVi05] T. Tao and M. Visan, *Stability of Energy-Critical Nonlinear Schrodinger Equations in High Dimensions*, Electronic Journal of Differential Equations **2005** (2005), no. 118, 1-28.

[TSVS24] K. Thulasidharan,<sup>1</sup> N. Sinhuja,<sup>2</sup> N. Vishnu Priya,<sup>3</sup> and M. Senthilvelan, *On examining the predictive capabilities of two variants of PINN in validating localised wave solutions in the generalized nonlinear Schrödinger equation*, arxiv 2407.07415v1

[Tsu87] Y. Tsutsumi,  *$L^2$ -solutions for nonlinear Schrödinger equations and nonlinear groups*. Funkcial Ekvac. 30: 115-25. 17, (1987).

[Val22] N. Valenzuela. *A new approach for the fractional Laplacian via deep neural networks*. Preprint arXiv:2205.05229 <https://arxiv.org/abs/2205.05229> (2022).

[Val23] N. Valenzuela, *A numerical approach for the fractional Laplacian via deep neural networks*, preprint arXiv:2308.16272 <https://arxiv.org/abs/2308.16272>, to appear in the 12th Computing Conference 2024 (London).

[WaYa21] L. Wang, Z. Yan, *Data-driven rogue waves and parameter discovery in the defocusing NLS equation with a potential using the PINN deep learning*, Phys. Lett. A 404, 127408 (2021).

[WWLL23] J. Wang, X. Wang, J. Li and B. Liu, *Data Generation-based Operator Learning for Solving Partial Differential Equations on Unbounded Domains*, arXiv:2309.02446

[XBC23] M. Xia 1, L. Böttcher, and T. Chou, *Spectrally adapted physics-informed neural networks for solving unbounded domain problems*, Mach. Learn.: Sci. Technol. 4 (2023) 025024.

[XCL21] C. Xie, J. Chen, and X. Li. *A machine-learning method for time-dependent wave equations over unbounded domains*. arXiv:2101.05807.

[Yar17] D. Yarotsky, *Error bounds for approximations with deep ReLU networks*, Neural Networks Volume 94, (2017), 103–114.

[ZYX22] Y. Zang, Z. Yu, K Xu, X Lan, M Chen, S Yang and H Chen, *Principle-driven Fiber Transmission Model based on PINN Neural Network*, Jour. Lightwave Technology Vol. 40(2), 404-414 (2022).

[ZhBa22] C.J. Zhang and Y.X. Bai, *A Novel Method for Solving Nonlinear Schrödinger Equation with a Potential by Deep Learning*. Jour.Appl. Math. Phys, 10, (2022) 3175-3190.

[Zer22] U. Zerbinati, *PINNs and GaLS: A Priori Error Estimates for Shallow Physics Informed Neural Networks Applied to Elliptic Problems*, IFAC-PapersOnLine Volume 55 (20), 61-66 (2022).

[ZFWCQ21] G-Zhou Wu, Y Fang, Y-Y Wang, G-Cheng Wu, C-Qing Dai, *Predicting the dynamic process and model parameters of the vector optical solitons in birefringent fibers via the modified PINN*, Chaos, Solitons & Fractals Volume 152: 111393, (2021).

[ZKCK22] W. Zhu, W. Khademi, E.G. Charalampidis, and P.G. Kevrekidis, *Neural Networks Enforcing Physical Symmetries in Nonlinear Dynamical Lattices: The Case Example of the Ablowitz-Ladik Model*. Physica D: Nonlinear Phenomena, 434:133264, (2022).

DEPARTAMENTO DE MATEMÁTICAS. UNIVERSIDAD DE CÓRDOBA, CÓRDOBA, SPAIN.

*Email address:* malejo@uco.es

IKERBASQUE AND UPV/EHU, APTDO. 644, 48080, BILBAO, SPAIN

*Email address:* lucrezia.cossetti@ehu.eus

IKERBASQUE & UNIVERSIDAD DEL PAÍS VASCO/EUSKAL HERRIKO UNIBERTSITATEA, UPV/EHU & BCAM, APTDO. 644, 48080, BILBAO, SPAIN

*Email address:* luca.fanelli@ehu.es

DEPARTAMENTO DE INGENIERÍA MATEMÁTICA AND CENTRO DE MODELAMIENTO MATEMÁTICO (UMI 2807 CNRS), UNIVERSIDAD DE CHILE.

*Email address:* cmunoz@dim.uchile.cl

DEPARTAMENTO DE INGENIERÍA MATEMÁTICA, UNIVERSIDAD DE CHILE.

*Email address:* nvalenzuela@dim.uchile.cl